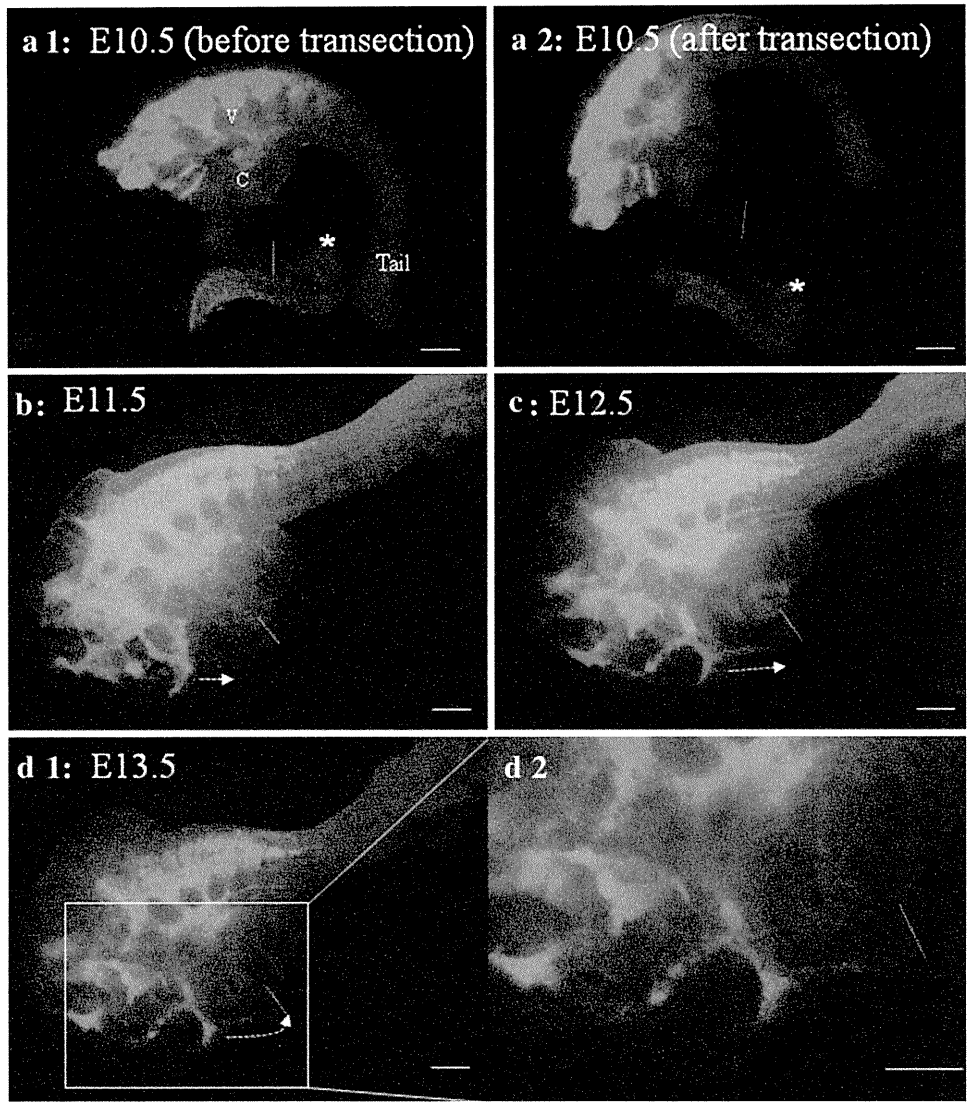

Fig. 1 Expression of V-positive NCC and extrinsic nerve fibers in transected bowel over time. On E10.5, the wavefront of V-positive vagal NCC has not yet reached the cecum (**a1**). After transection, no V-positive sacral NCC can be identified initially in the anorectum (**a2**). During day 1 of culture, thin V-positive nerve fibers can be observed dorsally (**b**). After 2 (**c**) to 3 (**d1**) days of culture, sacral NCC that are thick and beaded can be identified in the anorectum, and observed to migrate steadily, reaching the transected end. No V-positive vagal NCC are present. Original magnification ×2. **d2** high magnification of **d1** (original magnification ×4). The *white dotted line* indicates the line of transection. *Asterisk* indicates the cecum. The *dotted arrow* indicates the line of advancement of the proliferated thick extrinsic nerve fibers. *V* indicates vertebra. *C* indicates cloaca. *Scale bars* 200 μm. All images are composites of *fluorescent* and *dark* field images

neural crest lineage cells. The genotype of mice and fetuses were determined by a PCR protocol described elsewhere. The day a vaginal plug was detected was classified as embryonic day (E) 0.5. V-positive pregnant mice were sacrificed on E10.5 by cervical dislocation. Each embryo was harvested, the head removed and the body trimmed to leave distal ileum, colon, anorectum, sacrum, and tail. All animal procedures were reviewed and approved by the Juntendo University School of Medicine Animal Care and Use Committee (Institutional review board No.230033).

Tissue culture and image acquisition

Proximal colon of bowel from E10.5 embryos ($n = 10$) was transected at the ascending colon under M165FC FSM (Leica, Germany). Each transected specimen comprising distal colon, anorectum, and sacrum was placed in DMEM/F12 tissue culture medium (Gibco, USA), and images were taken at 24 h intervals. We observed the subsequent reaction of V-positive sacral NCC in the anorectum during organ culture, and compared them with non-transected control bowel specimens ($n = 10$). FSM was used to detect V, and data were processed with Adobe Photoshop.

Results

In E10.5 embryos, a wavefront of V-positive vagal NCC was observed and confirmed not to have reached the cecum (Fig. 1a1). In transected bowel specimens, no V-positive sacral NCC were identified initially in the anorectum (Fig. 1a2). However, during day 1 of culture, thin V-positive nerve fibers began to be observed dorsally (Fig 1b), and sacral NCC that were thick and beaded could be observed in the anorectum from about day 2 of cultivation in 6/10 (60 %) that proceeded to migrate steadily, reaching the transected end over the next 3–4 days (Fig. 1d1, d2). Thick beaded V-positive sacral NCC were

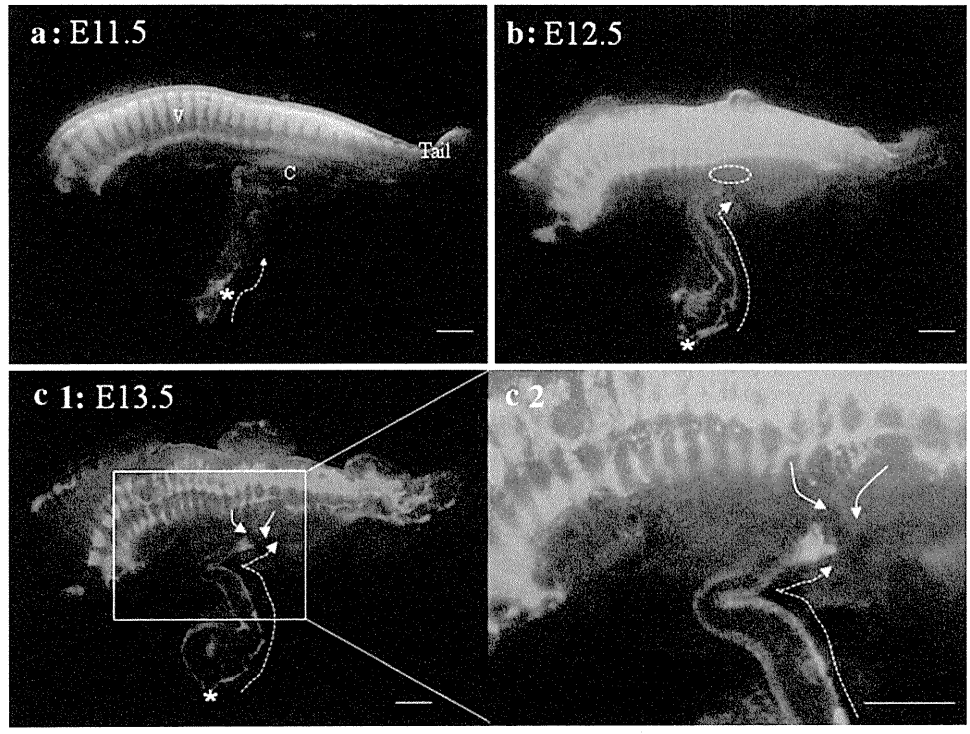

Fig. 2 Expression of V-positive NCC in control bowel over time. On E11.5, the wavefront of V-positive vagal NCC is present in the proximal colon (**a**). During day 1 of culture, V-positive vagal NCC migrated caudally. V-positive sacral NCC were not observed in the anorectum (*dotted circle*) (**b**). By day 2 of culture, V-positive sacral NCC began to migrate cranially and were met by distally migrating vagal NCC (**c1, c2**). Original magnification ×2, Scale bars 200 μm. **c2** high magnification of **c1**. Original magnification ×4.5, *Scale bars* 250 μm. *Asterisk* indicates the cecum. *Solid arrow* indicates the line of advancement of sacral NCC. *Dotted arrow* indicates the line of advancement of vagal NCC. All images are composites of *fluorescent* and *dark* field images

not observed to migrate from the anorectum in 4/10 (40 %) transected specimens. Control embryos were all approximately E11.5, and the wavefront of V-positive vagal NCC was confirmed in proximal colon (Fig. 2a). We were able to observe V-positive vagal NCC migrating caudally during day 1 of culture (Fig. 2b), and V-positive sacral NCC beginning to migrate cranially on day 2 of culture that were met by distally migrating vagal NCC; however, these V-positive sacral NCC were much thinner and shorter than those observed in transected bowel specimens (Fig. 2c1, c2).

Discussion

The enteric nervous system (ENS) is established by the migration of NCC along the gastrointestinal tract [8–13] necessitating extensive migration, proliferation, differentiation, and survival of enteric neurons and glial cells derived from the neural crest for normal ENS innervation to be established. Several studies have shown that there is rostral-to-caudal migration of vagal NCC that colonize the entire gut [8–13], in addition to caudal-to-rostral migration of sacral NCC that colonize a small terminal portion of the hindgut [13–16]. Knowing that there is failure of vagal NCC migration in the terminal hindgut that results in the absence of ganglion cells and proliferation of thick extrinsic nerve fibers in HD prompted us to think of some way to observe the behavior of sacral NCC when vagal NCC migration is disrupted. Our experimental technique allowed visualization of the proliferation of thick extrinsic nerve fibers in the aganglionic bowel in an artificial environment. In our model, we observed the migration of sacral NCC into the proximal colon with extending nerve fibers. Such nerves were not seen in control specimens in this study, and have not been reported previously in relation to normal gut development [13, 15, 16]. In fact, we did not observe any such reaction either in a recent study we published using SOX10-VENUS Tg [13].

The absence of ganglion cells and proliferation of thick extrinsic nerve fibers, i.e., hypertrophic nerves, in aganglionic bowel is pathognomonic for HD [17–19], but their exact etiology remains unknown. It has been assumed that proliferation of thick extrinsic nerve fibers occurs secondary to failure of vagal NCC reaching the terminal region of the hindgut. Various animal models for HD, such as chicks [14], rats [20], and mice [4–6, 16] have indicated that hypertrophic nerve fibers and an aganglionic segment result in the pathologic features of HD in humans [4–6], and the development of an aganglionic segment has been visualized directly using transgenic and knockout mouse. Similarly, we also used a mouse model for HD to show there is proliferation of thick extrinsic nerve fibers in aganglionic bowel [6]. Another study involving detailed observation in endothelin receptor B knockout mice, visualized thick extrinsic nerve fibers in the aganglionic segment advancing from pelvic ganglia (sacral NCC) cranially into the hypoganglionic region. [16]. Our results suggest that disruption of vagal NCC migration appears to induce sacral NCC activation in the anorectum, which

could have implications for the etiology of the thick nerve fibers seen in HD anorectum, which could in fact be a secondary phenomenon.

In the present study, proliferation of sacral nerve fibers were not noted in 40 % of transected bowel specimens. This could be a procedural problem, such as injury to the sacral NCC area due to stretching during transection and/or trimming. Further investigation is required to elucidate the causes and improve reproducibility.

Acknowledgments We are very grateful for technical support from the Division of Biomedical Imaging Research, BioMedical Research Center, Juntendo Graduate School of Medicine. Kawano Masanori Memorial Public Interest Incorporated Foundation for Promotion of Pediatrics provided funding support for this study.

References

1. Bodian M, Stephens FD, Ward BC (1949) Hirschsprung's disease and idiopathic megacolon. Lancet 1:6–11
2. Qualman SJ, Murray R (1994) Aganglionosis and related disorders. Hum Pathol 25:1141–1149
3. Watanabe Y, Ito F, Ando H et al (1998) Extrinsic nerve strands in the aganglionic segment of Hirschsprung's disease. J Pediatr Surg 33:1233–1237
4. Uesaka T, Nagashimada M, Yonemura S et al (2008) Diminished Ret expression compromises neuronal survival in the colon and causes intestinal aganglionosis in mice. J Clin Invest 118:1890–1898
5. Druckenbrod NR, Epstein ML (2009) Age-dependent changes in the gut environment restrict the invasion of the hindgut by enteric neural progenitors. Development 136:3195–3203
6. Miyahara K, Kato Y, Koga H et al (2010) Abnormal enteric innervation identified without histopathologic staining in aganglionic colorectum from a mouse model of Hirschsprung's disease. J Pediatr Surg 45:2403–2407
7. Shibata S, Yasuda A, Renault-Mihara F et al (2010) Sox10-Venus mice: a new tool for real-time labeling of neural crest lineage cells and oligodendrocytes. Mol Brain 3:31
8. Okamoto E, Ueda T (1967) Embryogenesis of intramural ganglia of the gut and its relation to Hirschsprung's disease. J Pediatr Surg 2:437–443
9. Le Douarin NM, Teillet MA (1973) The migration of neural crest cells to the wall of the digestive tract in avian embryo. J Embryol Exp Morphol 30:31–48
10. Okamoto E, Satani M, Kuwata K (1982) Histologic and embryologic studies on the innervation of the pelvic viscera in patients with Hirschsprung's disease. Surg Gynecol Obstet 155:823–828
11. Taraviras S, Pachnis V (1999) Development of the mammalian enteric nervous system. Curr Opin Genet Dev 9:321–327
12. Young HM, Bergner AJ, Anderson RB et al (2004) Dynamics of neural crest-derived cell migration in the embryonic mouse gut. Dev Biol 270:455–473
13. Miyahara K, Kato Y, Koga H et al (2011) Visualization of enteric neural crest cell migration in SOX10 transgenic mouse gut using time-lapse fluorescence imaging. J Pediatr Surg 46:2305–2308
14. Burns AJ, Champeval D, Le Douarin NM (2000) Sacral neural crest cells colonise aganglionic hindgut in vivo but fail to compensate for lack of enteric ganglia. Dev Biol 219:30–43
15. Wang X, Chan AK, Sham MH et al (2011) Analysis of the sacral neural crest cell contribution to the hindgut enteric nervous system in the mouse embryo. Gastroenterology 141(992–1002): e1001–e1006
16. Erickson CS, Zaitoun I, Haberman KM et al (2012) Sacral neural crest-derived cells enter the aganglionic colon of Ednrb-/- mice along extrinsic nerve fibers. J Comp Neurol 520:620–632
17. Huntley CC, Shaffner LD, Challa VR et al (1982) Histochemical diagnosis of Hirschsprung's disease. Pediatrics 69:755–761
18. Challa VR, Moran JR, Turner CS et al (1987) Histologic diagnosis of Hirschsprung's disease. The value of concurrent hematoxylin and eosin and cholinesterase staining of rectal biopsies. Am J Clin Pathol 88:324–328
19. Moore SW, Johnson G (2005) Acetylcholinesterase in Hirschsprung's disease. Pediatr Surg Int 21:255–263
20. Gariepy CE, Williams SC, Richardson JA et al (1998) Transgenic expression of the endothelin-B receptor prevents congenital intestinal aganglionosis in a rat model of Hirschsprung's disease. J Clin Invest 102:1092–1101

THE JOURNAL OF BIOLOGICAL CHEMISTRY VOL. 287, NO. 26, pp. 22205–22215, June 22, 2012

L-Sox5 and Sox6 Proteins Enhance Chondrogenic miR-140 MicroRNA Expression by Strengthening Dimeric Sox9 Activity*

Received for publication, January 16, 2012, and in revised form, April 11, 2012 Published, JBC Papers in Press, April 30, 2012, DOI 10.1074/jbc.M112.343194

Satoshi Yamashita[‡1], **Shigeru Miyaki**[§1], **Yoshio Kato**[¶], **Shigetoshi Yokoyama**[‡], **Tempei Sato**[‡‖], **Francisco Barrionuevo**[**], **Haruhiko Akiyama**[‡‡], **Gerd Scherer**[§§], **Shuji Takada**[‡], **and Hiroshi Asahara**[‡§‖¶¶2]

From the [‡]*Department of Systems Biomedicine, National Research Institute for Child Health and Development, 2-10-1 Okura, Setagaya-ku, Tokyo 157-8535, Japan, the* [§]*Department of Molecular and Experimental Medicine, The Scripps Research Institute, La Jolla, California 92037,* [¶]*Research Institute for Cell Engineering, National Institute of Advanced Industrial Science and Technology, Central 4, 1-1-1 Higashi, Tsukuba, 305-8562, Japan, the* [‖]*Department of Systems Biomedicine, Tokyo Medical and Dental University, 1-5-45 Yushima, Bunkyo-ku, Tokyo 113-8510, Japan, the* [**]*Department of Genetics, University of Granada, Center for Biomedical Research, Lab 127, Avda. Conocimiento s/n, ES-18100, Armilla, Granada, Spain, the* [‡‡]*Department of Orthopedics, Graduate School of Medicine, Kyoto University, 54 Kawahara-cho, Kyoto, 606-8507, Japan,* [§§]*Institute of Human Genetics, University of Freiburg, Breisacherstrasse, 33, D-79106 Freiburg, Germany, and* [¶¶]*Japan Science and Technology Agency, Core Research for Evolutional Science and Technology, Tokyo, Japan*

Background: miR-140 is a critical regulator of cartilage development and homeostasis.
Results: The proximal upstream region of miR-140 has *in vivo* chondrogenic promoter activity and an L-Sox5/Sox6/Sox9 (Sox trio) response element.
Conclusion: We reveal that L-Sox5 and Sox6 control miR-140 expression together with Sox9.
Significance: Uncovering molecular mechanisms of chondrogenesis has implications for cartilage repair and restoration of tissue function.

Sox9 plays a critical role in early chondrocyte initiation and promotion as well as repression of later maturation. Fellow Sox family members L-Sox5 and Sox6 also function as regulators of cartilage development by boosting Sox9 activation of chondrocyte-specific genes such as *Col2a1* and *Agc1*; however, the regulatory mechanism and other target genes are largely unknown. MicroRNAs are a class of short, non-coding RNAs that act as negative regulators of gene expression by promoting target mRNA degradation and/or repressing translation. Analysis of genetically modified mice identified miR-140 as a cartilage-specific microRNA that could be a critical regulator of cartilage development and homeostasis. Recent findings suggest Sox9 promotes miR-140 expression, although the detailed mechanisms are not fully understood. In this study we demonstrate that the proximal upstream region of *pri-miR-140* has chondrogenic promoter activity *in vivo*. We found an L-Sox5/Sox6/Sox9 (Sox trio) response element and detailed binding site in the promoter region. Furthermore, detailed analysis suggests the DNA binding and/or transactivation ability of Sox9 as a homodimer is boosted by L-Sox5 and Sox6. These findings provide new insight into cartilage-specific gene regulation by the Sox trio.

Chondrogenesis is executed in multiple steps during endochondral ossification. Mesenchymal cells condense, become immature chondroblasts, transform into prehypertrophic chondrocytes, and finally differentiate into hypertrophic chondrocytes (1). Extracellular matrix genes such as *Col2a1* and *Agc1* are expressed in the early stages; in the prehypertrophic and hypertrophic chondrocyte stages, however, their expression decreases, whereas *Col10a1*, *Ihh*, and *osteopontin* expression increases (2).

The HMG domain-containing transcription factor Sox9 plays a critical role in chondrogenesis except for hypertrophic chondrocyte formation (2, 3). Research with genetically modified mice further revealed that Sox9 initiates and promotes early chondrogenesis but suppresses the maturation stage (4–6). Sox9 recognizes the heptameric DNA sequence (A/T)(A/T)CAA(T/A)G and regulates chondrocyte-specific genes such as *Col2a1*, *Col11a2*, *CD-RAP*, *Agc1*, and *Hapln1* during cartilage development (7–12). Despite this role, molecular mechanisms have not been fully defined for Sox9 regulation of chondrogenesis.

Two other Sox family proteins play a critical role in cartilage development: L-Sox5, a long product of Sox5, and Sox6. L-Sox5 or Sox6 single knock-out mice exhibit a mild skeletal phenotype, whereas double knock-out mice show significant cartilage defects similar to Sox9 knock-out mice (4, 13). These proteins have a coiled-coil DNA-independent homodimerization domain but no other known functional domain (14). L-Sox5 and

* This work was supported, in whole or in part, by National Institutes of Health Grants AR050631 and AR056120. This work was also supported by Health and Labor Sciences research grants, grants-in-aid for Scientific Research (Ministry of Education, Culture, Sports, Science, and Technology of Japan), and Japan Science and Technology Agency, Core Research for Evolutional Science and Technology. This work was also supported by a grant from the Deutsche Forschungsgemeinschaft (to G. S.).
[1] Both authors contributed equally to this work.
[2] To whom correspondence should be addressed: 10550 North Torrey Pines Rd., La Jolla, CA 92037. Fax: 858-784-2695; E-mail: asahara@scripps.edu or 1-5-45 Yushima, Bunkyo-ku, Tokyo, 113-8510, Japan. Fax: +81-3-5803-5810; E-mail: asahara.syst@tmd.ac.jp.

Sox6 were found to boost Sox9 activity in regulating *Col2a1* expression; however, the regulatory mechanism is largely unknown as well as transcription targets beyond *Col2a1* and *Agc1* (8, 14).

MicroRNAs (miRNAs)[3] are a class of short (20–23 nucleotides), non-coding RNAs generated from primary transcripts (*pri-miRNAs*) by the action of Drosha and Dicer; they negatively regulate gene expression by promoting mRNA degradation and/or repressing translation through formation of RNA-induced silencing complexes and sequence-specific interaction with primarily 3′ untranslated regions on the target mRNA (15–17). Many miRNAs have tissue- and time-specific expression patterns determined at the *pri-miRNA* transcription level (18–20). Among known miRNAs, Tuddenham *et al.* (21) showed cartilage-specific expression of miR-140 in mouse embryos. We previously found that miR-140 expression was reduced in human osteoarthritis cartilage or in response to IL-1 stimulation, and miR-140-deficient mice exhibited short stature and age-related osteoarthritis symptoms (22, 23). These observations suggest that miR-140 plays a critical role in cartilage development and homeostasis. Recent findings indicate that Sox9 promotes miR-140 expression (24, 25), although detailed regulatory mechanisms are not fully understood.

We demonstrate in this study that the proximal upstream region of miR-140 has chondrogenic promoter activity *in vivo* and that cartilage-specific expression of miR-140 is generated from its specific transcript. We also reveal that L-Sox5 and Sox6 control miR-140 expression together with Sox9 through a response element in the promoter. Furthermore, detailed analysis suggests that the DNA binding and/or transactivation ability of Sox9 in its homodimer form is boosted by L-Sox5 and Sox6. The findings provide new insights into cartilage-specific gene regulation by this Sox trio.

EXPERIMENTAL PROCEDURES

Cell Culture, Transfection, and Adenovirus Infection—The human kidney cell line 293T and primary mouse chondrocytes were cultured in DMEM with 10% FBS at 37 °C. Primary chondrocytes were prepared from mouse embryo ribs (E16.5) and digested with collagenase. The 293T cell line was transfected using FuGENE HD transfection reagent (Promega). Sox9-expressing recombinant adenovirus was prepared for mouse chondrocytes using the adenovirus expression vector kit (Takara), and infection was performed according to manufacturer's instructions.

Reverse Transcription and Quantitative PCR—Total RNA was extracted with ISOGEN (Nippon Gene) according to the manufacturer's protocol and reverse-transcribed with SuperScript II (Invitrogen) and oligo(dT). Quantitative gene expression analysis was performed via real-time PCR using TaqMan Universal Master Mix reagents and TaqMan Probes (Applied Biosystems) on an ABI PRISM® 7900HT thermal cycler (Applied Biosystems). *Col2a1* and *Actb* were measured using the mouse TaqMan probes Mm00491889_m1 and Mm00607939_m1, respectively (Applied Biosystems). Data were normalized to *Actb* gene expression for each experiment. Quantitative miRNA expression analysis was performed using the TaqMan MicroRNA reverse transcription kit and TaqMan MicroRNA assay (Applied Biosystems). miR-140 expression was measured using the TaqMan probe TM001187, and *snoRNA202* (TM001232) expression was used as an internal control to normalize differences in each sample.

Rapid Amplification of cDNA Ends (RACE)—Total RNA and mRNA were isolated from chondrocytes with TRIzol (Invitrogen) and OligotexdT30 (Takara). 5′- and 3′-RACE were performed using the GeneRace kit (Invitrogen) with region-specific primers (5′ RACE primer (5′-CGATGCAGAGGGTGCTCCAGTACCCTGTCCGTG-3′), 5′ RACE nested primer (5′-CCGTGGTTCTACCCTGTGGTAGAACAGCATGACGT-3′), 3′ RACE primer (5′-ACCCTATGGTAGGTTACGTCATGCTGTTCTACCACAGGG-3′), and 3′ RACE nested primer (5′-ACGTCATGCTGTTCTACCACAGGGTAGAACCACGG-3′).

RNA in Situ Hybridization—Whole mount and section *in situ* hybridization was performed as previously described (26). Gene-specific fragments were amplified from mouse chondrocyte cDNA by PCR with primers (*pri-miR-140*, forward 5′-TGGTGTGTGGTTCTATGCCAGC-3′ and reverse 5′-AGCCTCAAGCCAGAATTCAGG-3′; *Sox9*, forward 5′-TTGAGACCTTCGACGTCAATGAG-3′ and reverse 5′-TCTGGCCACGAGTGGCC-3′). The *Col2a1* probe sequence was described in a previous study (27).

Sox9 Conditional Knock-out Mice—In embryos with *Sox9*, conditional knock-out mice were generated as described using *CK-19 Cre* and *Col2a1 Cre* transgenic mice (4, 28).

Reporter Assay—The pGL4.12 vector (Promega), including indicated cloned genome regions, and the indicated gene expression vector were transfected into 293T cells. The *Renilla* luciferase reporter pRL-TK (Promega) was co-transfected as a control to evaluate transfection efficiency. Cells were lysed, and luciferase activity was measured with the Dual-Glo™ Luciferase Assay System (Promega). Data were normalized to *Renilla* luciferase activity for each experiment. Mutations were introduced with QuikChange® site-directed mutagenesis (Stratagene) according to the manufacturer's instructions.

Generation of miR140 Promoter-LacZ Transgenic (Tg) Mice—To generate miR-140 promoter-LacZ Tg mice, an upstream region of miR-140 was amplified by PCR from mouse genome DNA using specific transgene primers (forward, 5′-ACTGTTCAGAAGGAGACTACTCTGTC-3′; reverse, 5′-ACCGACCTCTGCTCAGCTC-3′). The amplified fragment was cloned into a vector containing the LacZ gene, and Tg BDF1 mice were generated with pronuclear injection of the transgene. Tg mice were confirmed by PCR analysis of genomic DNA using specific transgene primers (forward, 5′-GGTGCTTTGTGAAGGGAAAG-3′; reverse, 5′-GTTGCACCACAGATGAAACG-3′).

X-Gal Staining—LacZ expression from miR140-LacZ Tg mice was detected by X-gal staining. Whole mount Tg embryos were incubated in fixation solution (1% paraformaldehyde, 0.2% glutaraldehyde, and 0.02% Nonidet P-40 in PBS) for 30 min at room temperature. The embryos were then washed with

[3] The abbreviations used are: miRNA, microRNA; RACE, rapid amplification of cDNA ends; Tg, Transgenic; TSS, transcriptional start site; PSB, putative Sox binding.

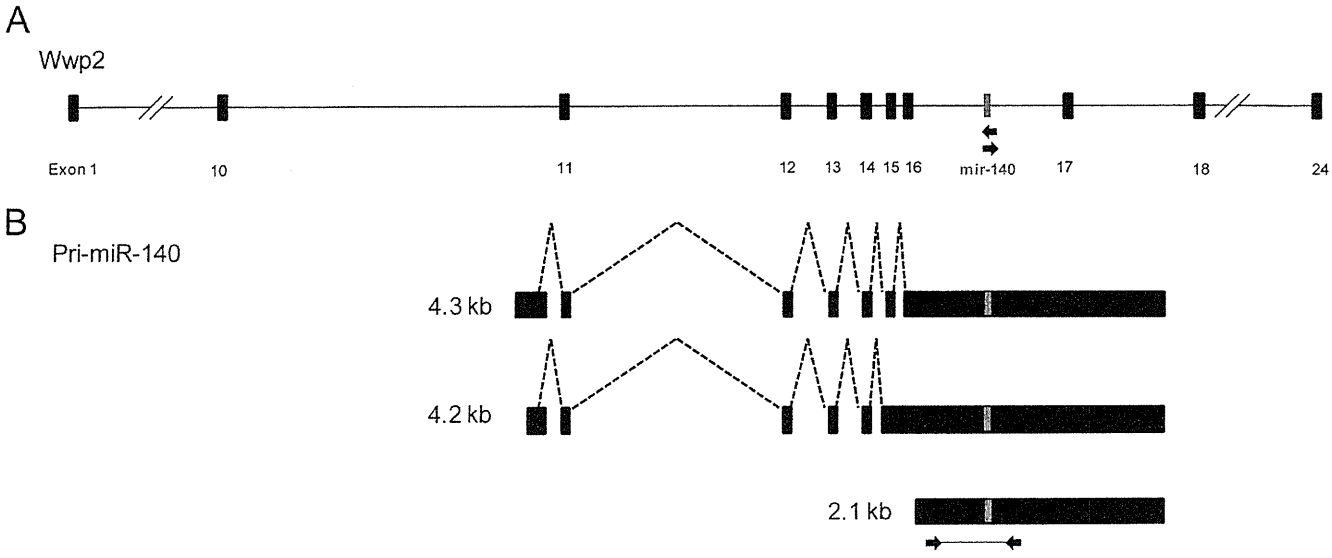

FIGURE 1. **Three isoforms were detected for *pri-miR-140*.** *A*, miR-140 is located on chromosome 8 and intron 16 of the WW domain containing E3 ubiquitin protein ligase 2 (*Wwp2*) gene. *B*, three different-sized transcripts were identified for *pri-miR-140* from 5′- and 3′-RACE performed using the primers indicated with *arrows* in *A*. The *pri-miR-140* probe used for *in situ* hybridization is indicated with *arrows* in *B*.

1 mM $MgCl_2$ in PBS and stained with staining solution (0.01% sodium deoxycholate, 0.02% Nonidet P-40, 1 mM $MgCl_2$, 5 mM potassium ferricyanide, 5 mM potassium ferrocyanide, and 0.1% X-gal in PBS) overnight at 37 °C.

Electrophoretic Mobility Shift Assay (EMSA)—DNA-protein binding was assayed with DNA probes ^{32}P-radiolabeled by end-filling with Klenow fragment and luciferase or Sox9 with or without anti-Sox9 antibodies. Reactions were carried out at 25 °C for 30 min in binding buffer (20 mM HEPES (pH 7.9),10% glycerol, 50 mM KCl, 0.05% Nonidet P-40, 0.5 mM EDTA, 0.5 mM DTT, and 1 mM PMSF) and 0.5 μg of poly(dG-dI), a non-specific competitor. Anti-Sox9 antibody was preincubated with Sox9 for 30 min at 25 °C before the addition of the radiolabeled probes. Binding reactions were separated by PAGE on a 4% gel for 3 h at 100 V. Proteins were synthesized *in vitro* with the TNT T7 Quick Coupled Transcription/Translation System (Promega) and each expression plasmid.

Chromatin Immunoprecipitation (ChIP)—ChIP was performed as previously described (29). Briefly, cells were cross-linked with 1% formaldehyde for 15 min at room temperature before glycine was added for a final concentration of 0.125 M. Chromatin was sheared to ~200–1000 bp by sonication. The chromatin solution was then incubated with the indicated antibodies bound to Dynabeads® Protein A (Dynal Biotech) at 4 °C. Sox9 (Millipore), Sox5 (Abcam, ab94396), and Sox6 (Abcam, ab30455) antibodies were used, with normal rabbit IgG antibodies (Santa Cruz Biotechnology, Inc.) as negative controls. Immune complexes were eluted from the beads and reverse-cross-linked at 65 °C. Chromatin-immunoprecipitated DNA was purified using the MinElute PCR purification kit (Qiagen) and analyzed with whole cell extract by real-time PCR with specific primers (miR140-PSB, forward 5′-GTATTTGCACA-AGGCTGGAC-3′ and reverse 5′-AGACCTGGCTGGCTC-CAT3′; miR140-Far Ups, forward 5′-CTATCTACC-CGGGCCACCTG-3′ and reverse 5′-GGACCTATGC-TGGGACAATC-3′).

RESULTS

Chondrogenic Expression of miR-140 Is Regulated by Sox9—miR-140 is located in intron 16 of the WW domain containing E3 ubiquitin protein ligase 2 (*Wwp2* gene) and consists of an N-terminal C2 domain, a C-terminal HECT domain, and four WW domains in the center (Fig. 1*A*). To determine the transcriptional start site (TSS) and 3′ end of *pri-miR-140*, we performed 5′- and 3′-RACE using mRNA from cultured mouse chondrocytes. We detected three different transcripts with the miR-140 sequence (Fig. 1*B*). The shortest was 2.1 kb long, starting inside intron 16. The two longer transcripts were splice variants 4.2 and 4.3 kb long, with the same TSS inside intron 10. All three isoforms had the same 3′ end.

miR-140 expression has been previously detected in the primordia of future bones and across the autopod, zeugopod, and stylopod of E11.5 mouse embryo forelimbs and hind limbs with a mature miR-140 LNA oligonucleotide probe (21). Still, precise temporal and spatial miR-140 expression patterns have not been characterized during chondrogenesis. To explore miR-140 expression further, we performed *in situ* hybridization using an RNA probe for *pri-miR-140* common to all three isoforms (Fig. 1*B*). The expression pattern in the cartilage of E11.5 embryos was similar to the chondrocyte differentiation markers *Sox9* and *Col2a1*, a target gene of Sox9 (Fig. 2, *A–F*). *Sox9* and miR-140 expressions were also similarly detected in the cartilage of digits from E11.5 to E14.5 (Fig. 2, *G* and *H*).

Our *in situ* hybridization analysis found that miR-140 expression resembled *Sox9* and one of its target genes, *Col2a1* expression in limb buds, which suggests the possibility that Sox9 regulates miR-140 expression in limb development. To test this hypothesis, we examined the effect of repressing Sox9 expression on miR-140 expression. *Sox9flox/flox;Ck19-Cre* embryos abolish Sox9 expression before mesenchymal condensation, and chondrogenic cell lineage commitment is profoundly impaired as a consequence (28). In E12.5 wild type and

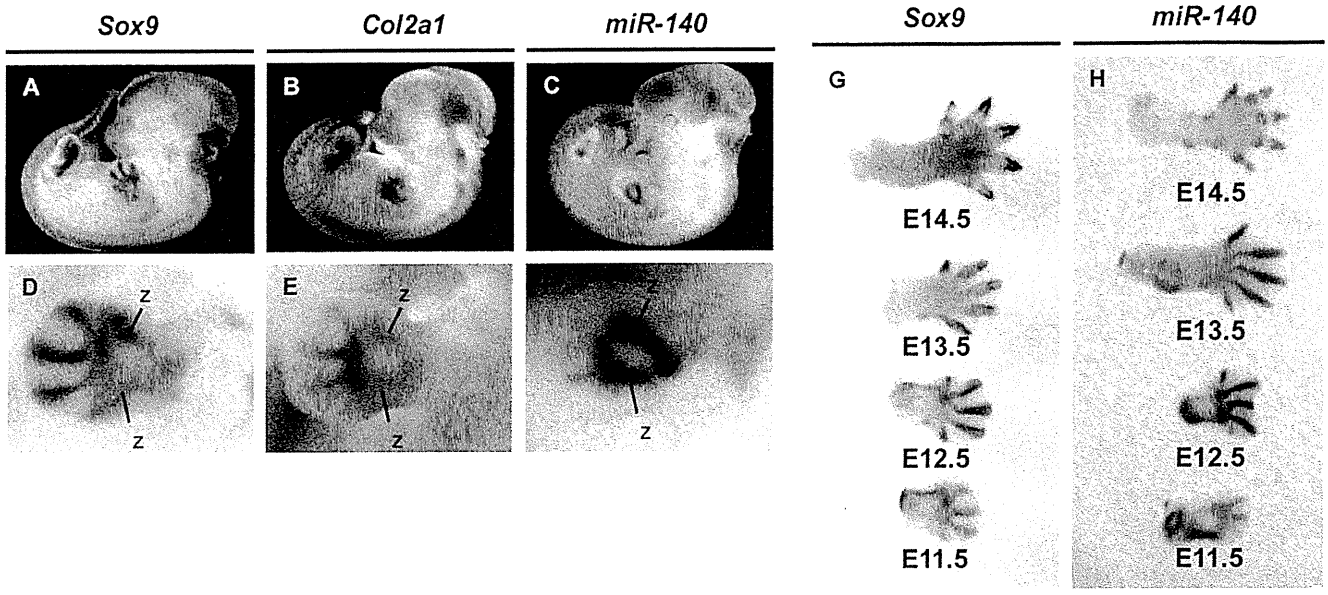

FIGURE 2. **Cartilage-specific expression of *pri-miR-140* in mouse embryos.** Shown is a comparison of *Sox9* (*A* and *D*), *Col2a1* (*B* and *E*), and *pri-miR-140* (*C* and *F*) expression patterns in mouse whole mount embryos and developing mouse forelimb buds at embryonic stage E11.5. Zeugopod elements are indicated as *z*. Shown is the Sox9 (*G*) and *Pri-miR-140* (*H*) expression pattern in the cartilage of developing digits during E11.5 to E14.5.

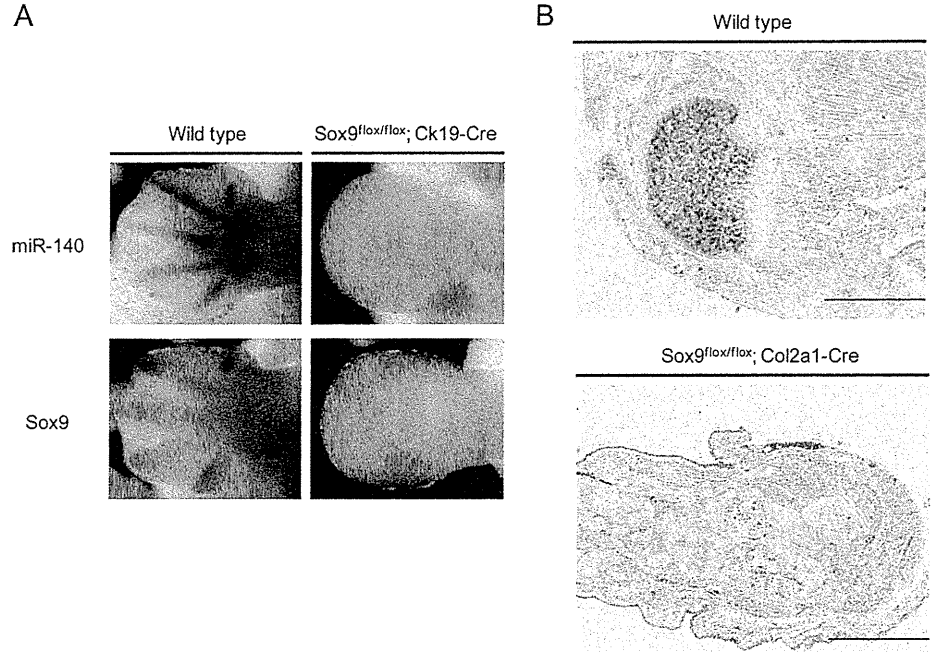

FIGURE 3. **Pri-miR-140 expression is reduced in Sox9-deficient mouse limb buds and chondrocytes.** *A*, *Pri-miR-140* and Sox9 expression patterns in the forelimb buds of wild type and *Sox9flox/flox;Ck19-Cre* mouse embryos at E12.5 are shown. Expression of both transcripts was drastically reduced in mutant embryos. *B*, *Pri-miR-140* expression was detected in wild type femurs at E16.5 but not E16.5 *Sox9flox/flox;Col2a1-Cre* femurs.

Sox9flox mice without Cre expression, the miR-140 expression pattern overlapped with the Sox9 pattern (Fig. 3*A*, *left*). Expression of *pri-miR-140* in Sox9 mutant cells at E12.5 was completely absent, however, as was Sox9 expression (Fig. 3*A*, *right*). These results suggest that Sox9 is a regulator of miR-140, but there is a possibility that the absence of miR-140 expression in the *Sox9flox/flox;Ck19-Cre* embryo limb buds was the result of absent chondrogenic lineage cells from impaired chondrogenic mesenchymal condensation. We thus examined *Sox9flox/flox; Col2a1-Cre* embryos, where Sox9 was inactivated in condensed mesenchymal cells and differentiated chondrocytes through *Col2a1-Cre*-mediated recombination (4). In E16.5 wild type embryos, *pri-miR-140* was expressed in the proliferating chondrocyte zone but absent in the hypertrophic zone (Fig. 3*B*, *top*). In contrast, miR-140 was completely absent in condensed chondrogenic mesenchymal cells and differentiated chondrocytes from *Sox9flox/flox; Col2a1-Cre* embryos (Fig. 3*B*, *bottom*). This shows that Sox9 dominates regulation of miR-140 expression in differentiating chondrocytes *in vivo*.

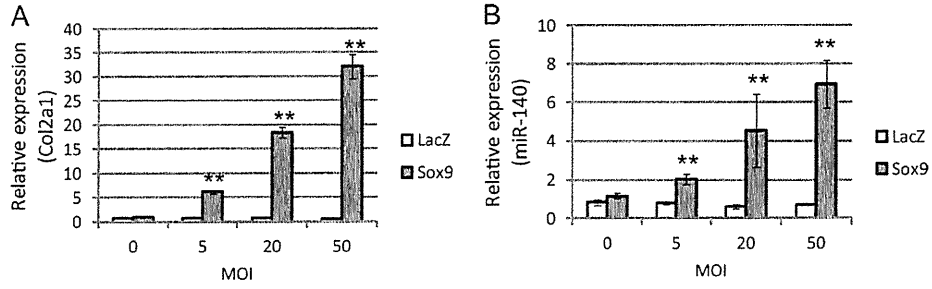

FIGURE 4. **miR-140 expression is up-regulated by Sox9 in chondrocytes.** LacZ-expressing adenoviruses as a negative control or Sox9-expressing adenoviruses were transduced into cultured mouse chondrocytes with incremental multiplicities of infection (*MOI*). *Col2a1* mRNA (*A*) and miR-140 (*B*) expression after Sox9 overexpression were evaluated with quantitative PCR. Data are presented as the mean ± S.D.; $n = 3$. Statistical differences were calculated using the *t* test. **, $p < 0.01$

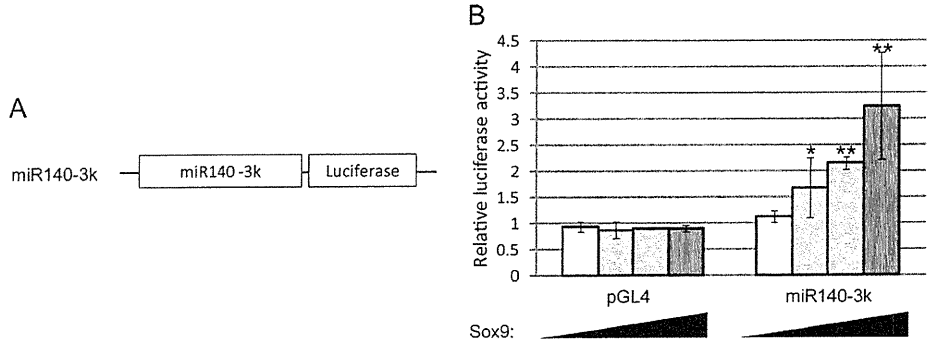

FIGURE 5. **miR-140 proximal promoter activity is up-regulated by Sox9.** *A*, shown is a luciferase reporter construct containing a 3-kb proximal upstream region of *pri-miR-140*. *B*, 293T cells were co-transfected with pGL4 as a negative control or the miR140–3k reporter plasmid and increasing amounts of Sox9-expressing plasmid (0, 50, 100, and 400 ng). Luciferase activity is presented as the mean ± S.D.; $n = 3$. Statistical differences were calculated using *t* test. *, $p < 0.05$; **, $p < 0.01$.

We also studied the effect of Sox9 overexpression on miR-140 expression through quantitative PCR analysis for cultured chondrocytes. Adenovirus infection-mediated Sox9 overexpression increased miR-140 expression as well as *Col2a1* expression and correlated with increased multiplicity of infection; adenovirus infection-mediated LacZ overexpression did not affect miR-140 expression (Fig. 4, *A* and *B*). Taken together, the results from all these experiments indicate that miR-140 expression is up-regulated by Sox9 in chondrocytes and developing limbs.

Upstream Region of miR-140 Is Critical for Its Chondrogenic Expression and Sox9 Regulation—To determine a direct regulatory mechanism for miR-140 expression by Sox9, we constructed a reporter plasmid with a 3-kb region upstream from the miR-140 TSS and a luciferase gene (miR140–3k). With the reporter plasmid and increasing amounts of Sox9-expressing plasmids, luciferase activity in 293T cells increased in a dose-dependent manner (Fig. 5). Sox9 thus regulates miR-140 expression by activating a promoter region 3 kb upstream of its TSS.

Another reporter plasmid with the 3-kb region upstream of miR-140 and a *LacZ* gene (Fig. 6*A*) was prepared and used to generate transgenic (Tg) mice (miR140–3k-LacZ). We generated three lines of transgenic mice, and all of those transgenic E12.5 and E15.5 embryos revealed LacZ expression in forelimbs, hind limbs, and other cartilage tissue such as ribs and vertebrae with an expression pattern similar to miR-140 (Fig. 6, *B–E*). These *in vitro* and *in vivo* results suggest that miR-140 expression in limb development and cartilaginous tissues is regulated by a 3-kb region upstream of its TSS and promoted by Sox9.

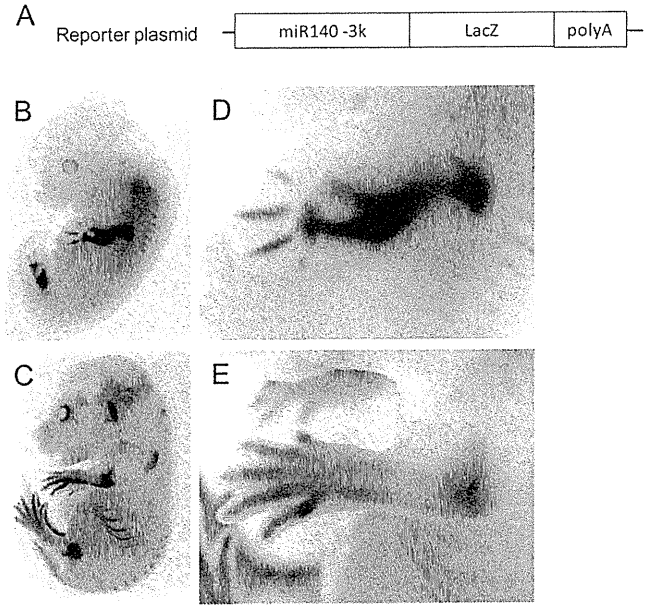

FIGURE 6. **The miR-140 proximal promoter has chondrogenic activity.** *A*, shown is an LacZ construct containing a 3-kb upstream region of *pri-miR-140* transgene. LacZ expression patterns in miR140–3k-LacZ transgenic (Tg) mouse embryos at E12.5 (*B*) and E15.5 (*C*). Shown is a magnified view of forelimb at E12.5 (*D*) and E15.5 (*E*).

Sox9 Binds to Upstream Region of miR-140 and Enhances Its Expression in Concert with L-Sox5 and Sox6—Previous studies have clarified that L-Sox5 and Sox6 are critical regulators of

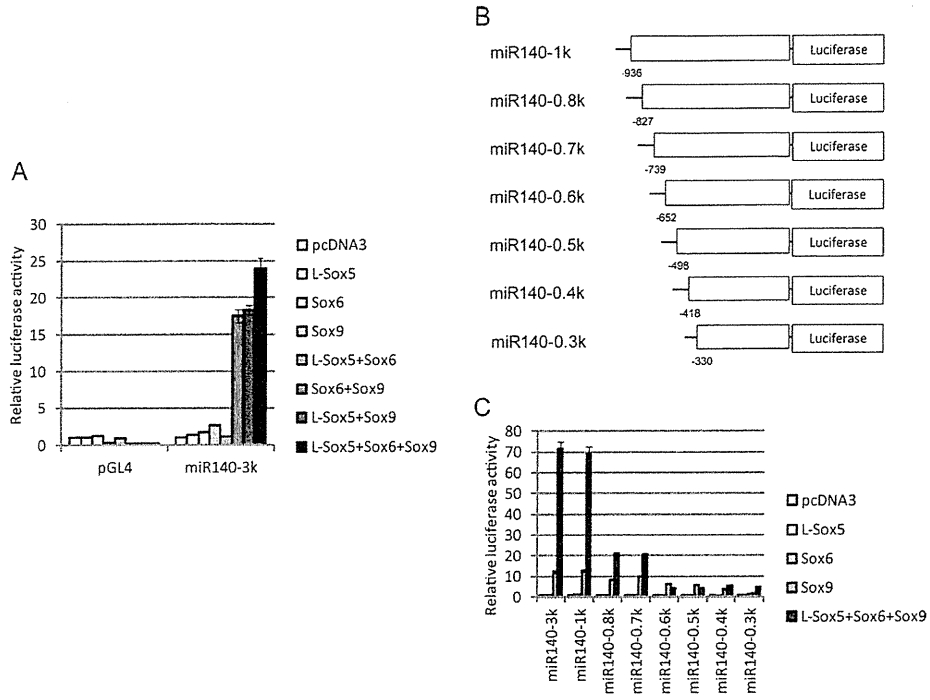

FIGURE 7. **L-Sox5 and Sox6 enhance Sox9-dependent proximal promoter activation of miR-140.** *A*, 293T cells were co-transfected with pGL4 as a negative control or with the miR140–3k reporter plasmid and the indicated expression plasmids. Luciferase activity is presented as the mean ± S.D.; $n = 3$. *B*, luciferase reporter constructs containing different lengths of the miR-140 upstream region are shown. *Numbers* indicate position from the *pri-miR-140* transcription start site. *C*, luciferase activity using the reporter plasmids displayed in *B* and indicated expressing plasmids is presented as the mean ± S.D.; $n = 3$.

chondrogenesis and function as Sox9 co-operators in chondrocytes (4, 14). It has also been reported that expression of chondrogenic genes regulated by Sox9, such as *Col2a1* and *Agc1*, is enhanced by L-Sox5 and Sox6 (8, 14). Therefore, we explored whether L-Sox5 and Sox6 were involved with Sox9 in regulation of miR-140 expression.

We first examined promoter activity from the miR140–3k reporter plasmid coupled with overexpression of L-Sox5, Sox6, and/or Sox9 in 293T cells. Luciferase activity was greater with overexpression of the Sox trio than with Sox9 alone, and L-Sox5 and/or Sox6 did not enhance activity without Sox9 overexpression (Fig. 7*A*). L-Sox5 and Sox6 can thus promote miR-140 expression through activating Sox9.

A series of deletion constructs in the miR-140 upstream region was then created to identify the Sox trio response element (Fig. 7*B*). Luciferase activity up-regulated by the Sox trio decreased with a deletion from −936 to −827 bp upstream of the miR140 TSS and was almost abolished with a deletion from −739 to −652 bp (Fig. 7*C*). Remarkably, an additional increase in activity by L-Sox5 and Sox6 co-transfected with Sox9 was not shown with deletion of the −739 to −652 bp upstream region (Fig. 7*C*).

Our luciferase assay analysis indicates that the −739 bp upstream region from miR-140 TSS is minimally required for its regulation by L-Sox5, Sox6, and Sox9 (Sox trio). We then constructed a LacZ reporter plasmid containing −739 bp upstream region from miR-140 TSS (Fig. 8*A*) and generated Tg mice (miR140–0.7k-LacZ) to examine whether the minimal region is essential for its chondrogenic expression. We observed that the four other miR140–0.7k-LacZ mice expressed LacZ in cartilaginous tissues that expression was similar to

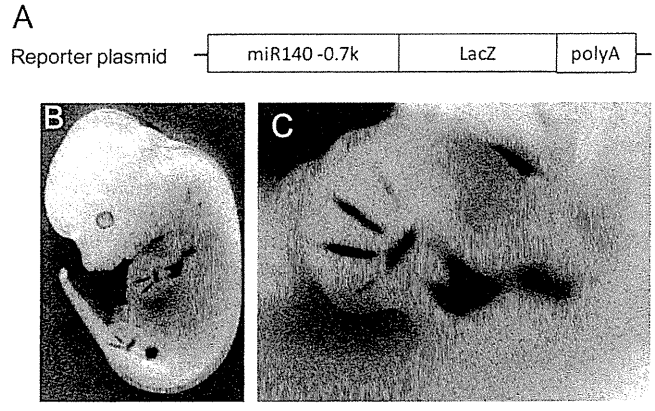

FIGURE 8. **The 0.7-kb upstream region of miR-140 has chondrogenic promoter activity.** *A*, shown is the LacZ reporter construct containing −739 bp upstream region of *pri-miR-140* transgene. *B*, shown are LacZ expression patterns in miR140–0.7k-LacZ Tg mouse of E12.5 embryos. *C*, shown is a magnified view of forelimb.

miR140–3k-LacZ mice (Fig. 8, *B* and *C*). These results indicate that the −739-bp proximal upstream region of miR-140, which is minimally required for its regulation by Sox trio, is essential for its chondrogenic expression.

The −739 to −652-bp upstream region was then explored in detail because up-regulation by the Sox trio was abolished with its deletion. We looked for consensus Sox9 binding sequences because Sox trio up-regulation was still Sox9-dependent and found a putative imperfect palindromic sequence in the binding site (Fig. 9*A*). Previous reports indicated that Sox9 homodimers bind to enhancer regions that contain inverted Sox9 binding sites separated by 3–4 bp and represent a palindromic motif for chondrocyte-specific gene regulation (30–32). To assess

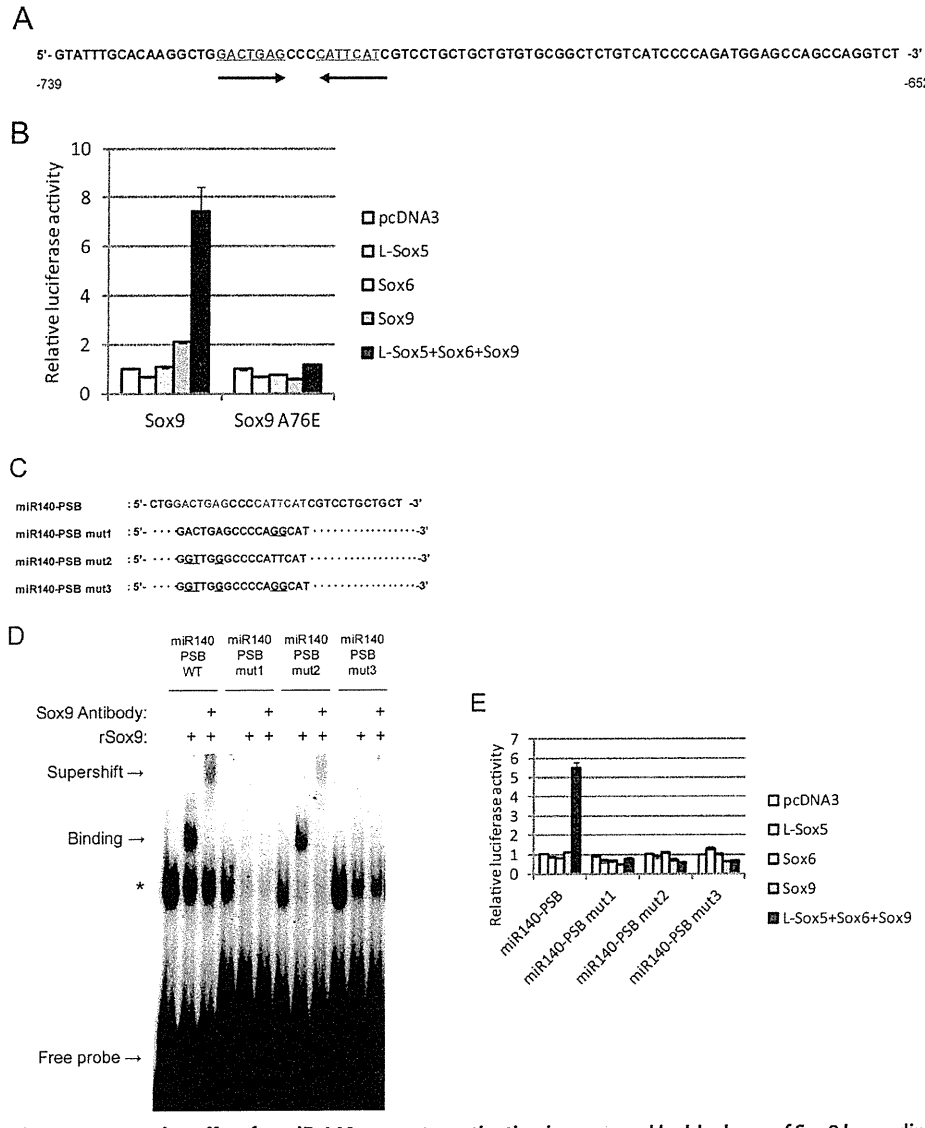

FIGURE 9. **The L-Sox5 and Sox6 cooperative effect for miR-140 promoter activation is repressed by blockage of Sox9 homodimer formation.** *A*, shown is a sequence of the region −739 and −652 bp upstream from the *pri-miR-140* transcription start site. A putative Sox9 binding site is indicated in *red*; *arrows* indicate site orientation. *B*, 293T cells were co-transfected with the miR140 – 0.7k reporter plasmid displayed in Fig. 7*B* and the indicated expressing plasmids. Wild type Sox9 (*left*) or Sox9 with a dimerization missense mutation (A76E) (*right*) were used as expression plasmids. Luciferase activity is presented as the mean ± S.D.; $n = 3$. *C*, shown are wild type and mutant oligonucleotide probe sequences corresponding to Sox9 binding sites in the miR-140 promoter. *D*, binding of oligonucleotide probes with wild type and mutated PSB consensus sequences complexed to recombinant Sox9 protein (*rSox9*) was detected by electrophoretic mobility shift assay. Mutations in one (*mut1*, *mut2*) or both (*mut3*) Sox9 binding motifs were compared with the wild type (*WT*) in the presence or absence of anti-Sox9 antibody. *E*, 293T cells were co-transfected with reporter plasmids containing the −739- and −652-bp *pri-miR-140* wild type upstream region (*miR140-PSB*) or the mutations displayed in C and the indicated expressing plasmids. Luciferase activity is presented as the mean ± S.D.; $n = 3$.

whether Sox9 homodimer binding was critical for miR-140 regulation, a miR140 – 0.7k reporter construct and Sox9 A76E expression plasmid that does not form homodimers were used (30–32). There was no obvious up-regulation of luciferase activity by Sox9 A76E alone or with co-expression in the Sox trio, in contrast to the Sox9 wild type plasmid (Fig. 9*B*). To confirm that Sox9 binds to the putative palindromic sequence, we performed EMSA using oligonucleotide probes for the putative Sox binding (PSB) sequences (Fig. 9*C*). miR140-PSB probes detected a band when incubated with recombinant Sox9 protein, and additional incubation with anti-Sox9 antibody reduced the band with an upward supershift (Fig. 9*D*). Utilizing probes with point mutations in one or both Sox9 binding sequences (Fig. 9*C*) resulted in band reduction, where miR140-PSB mut1 almost abolished the band, and mutations in both motif sites completely abolished the band (Fig. 9*D*). The same results occurred with the supershift band produced by incubation with anti-Sox9 antibody (Fig. 9*D*). To further confirm Sox9 binding and promoter activity in the −739 ~ −652-bp region upstream of the miR-140 TSS, another luciferase reporter assay was performed with a vector containing point mutations in one or both Sox9 motif sites. Dual mutations and a single Sox9 motif mutation diminished up-regulation of promoter activity by Sox trio expression (Fig. 9*E*).

Finally, the ability of Sox9 to bind to the endogenous miR-140 promoter was examined in E13.5 mouse limbs by a ChIP

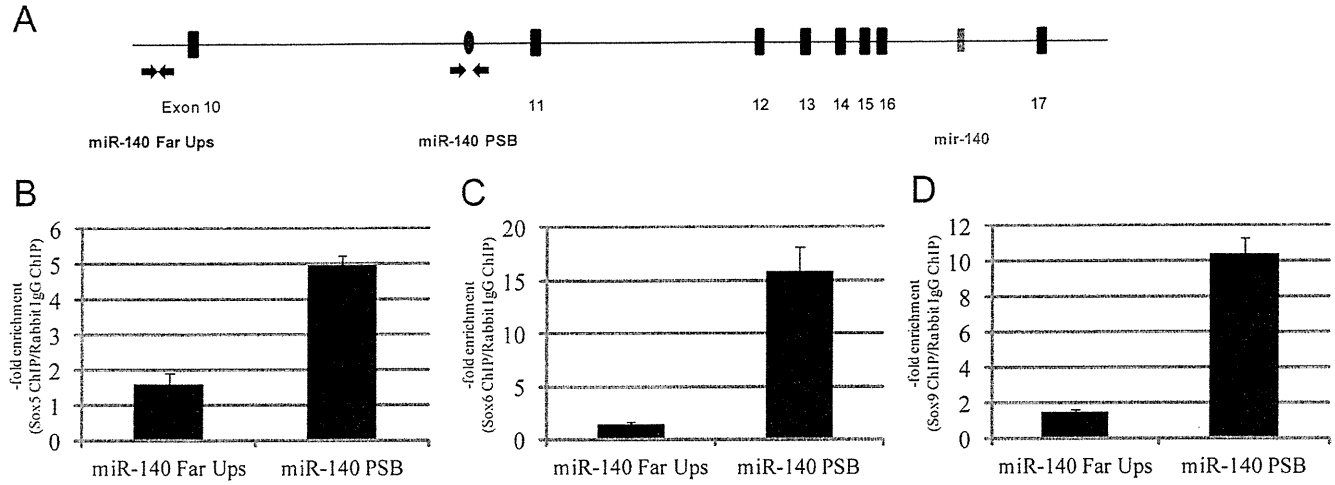

FIGURE 10. **The Sox trio binds to the miR-140 promoter in E13.5 mouse limbs.** *A*, location of site-specific primer sets for PSB sites and the −5 kb upstream (*Far Ups*) region of the *pri-miR-140* TSS as a negative control are displayed by *arrows*. *B*, chromatin-immunoprecipitated DNA and whole cell extract DNA in E13.5 mouse limbs were quantitatively analyzed by real-time PCR. The enrichment value of L-Sox5 (*B*), Sox6 (*C*), and Sox9 (*D*) chromatin-immunoprecipitated DNA was calculated by dividing rabbit IgG chromatin-immunoprecipitated DNA data as a negative control. Data are presented as the mean ± S.D.; $n = 3$.

assay using far upstream (approximately −5 kb) (miR140 Far Ups) and putative Sox9 binding site (miR140 PSB) primer sets as shown in Fig. 10*A*. The enrichment value of the putative Sox9 binding site was confirmed in Sox9 chromatin-immunoprecipitated DNA, although the far upstream site did not show enrichment (Fig. 10*B*). Additionally, the use of antibodies showed that L-Sox5 and Sox6 also bound to the putative Sox9 binding site but not the far upstream site (Fig. 10, *C* and *D*). Taken together, these results suggest that Sox9 enhances miR-140 expression by cooperating with L-Sox5 and Sox6 to bind −739 ~ −652 bp upstream from the miR-140 TSS.

DISCUSSION

Most miRNAs, which frequently are located within the intron region of genes, originate from the spliced intronic RNA of a host gene transcript (33). The cartilage-specific intronic miRNA miR-140 is located in intron 16 of *Wwp2*, a host gene that functions as a critical regulator of craniofacial development and is also expressed in cartilaginous tissues (34, 35). *Wwp2* expression is directly regulated by the binding of Sox9 to intron 3 (35), which suggests that miR-140 expression can be similarly generated and regulated from the *Wwp2* transcript. In this study we demonstrated that the proximal upstream region of *pri-miR-140* located in intron 10 of *Wwp2* has *in vivo* promoter activity. The results suggest that miR-140 may be derived from its own specific transcript during chondrogenesis.

Previous studies found miR-140 to be specifically expressed in chondrocytes and a critical regulator of cartilage development and homeostasis (21–23). Our *in situ* hybridization analysis confirmed that *pri-miR-140* expression was chondrocyte-specific in mouse embryos and mirrored Sox9 expression patterns as shown in limb buds. Also, miR-140 expression was abolished in Sox9-deficient limb buds and chondrocytes and enhanced in cultured chondrocytes with overexpressed Sox9. These findings show that Sox9 is a direct regulator of miR-140 as well as *Wwp2*. A recent study indicated that Sox9 binds to intron 10 of *Wwp2* and up-regulates miR-140 expression (25). By further exploring this mechanism, we found that Sox9 activates a promoter region upstream of miR-140 on intron 10 with *in vivo* chondrogenic activity. This strongly suggests that miR-140 *in vivo* chondrogenic expression is directly regulated in part through activation of its promoter region by Sox9 instead of splicing itself out of the host transcript.

Most previously known Sox9 targets were extracellular matrix genes, and only a few, such as *Bapx1*, *S100A1*, and *S100B*, were shown to be direct regulators of it except for extracellular matrix genes (29, 36). Our *in vivo* and *in vitro* analyses demonstrated that miR-140 is also a downstream target of Sox9. Previous studies reported that miR-140 repressed Hdac4 to block chondrocyte maturation, Adamts-5 to promote cartilage development and homeostasis, and Sp1 to maintain chondrocyte proliferation (21, 23, 25). These diverse roles are similar to Sox9, which also promotes early chondrogenesis but represses chondrocyte maturation (2). Furthermore, Sox9 expression was significantly lower in osteoarthritis cartilage compared with normal cartilage (37), whereas miR-140 knockout mice exhibited age-related, osteoarthritis-like phenotypes (23). These studies strongly support miR-140 as both a downstream and a critical target of Sox9 due to its diverse roles in chondrogenesis. In fact, miR-140-deficient mice have a mild skeletal phenotype with a short stature (23).

In this study we showed that L-Sox5 and Sox6 were also involved in regulation of miR-140 expression with Sox9. Results showed that expression levels did not change in the presence of L-Sox5 and/or Sox6 without Sox9 co-expression, making control of miR-140 expression by L-Sox5 and Sox6 completely Sox9-dependent. L-Sox5 and Sox6 participate in the regulation of cartilage-specific genes such as *Col2a1* and *Agc1*, although they have no known transactivation or transrepression domains (8, 14). A recent study suggested that L-Sox5 and Sox6 may facilitate Sox9 DNA binding by an unknown mechanism (8). A comparable regulatory event by the Sox trio may also occur with the miR-140 promoter.

Our detailed luciferase, EMSA, and ChIP analyses identified the precise Sox trio response element and Sox9 binding site.

Sox9 was previously reported as bound to intron 10 of *Wwp2* to regulate miR-140 expression (25). However, the Sox9 binding site exhibited in this study is different and suggests the possibility that miR-140 expression is controlled by multiple Sox9 and/or the Sox trio binding in its promoter region, as shown with *Col11a2* expression that is directed by Sox9 at least three cartilage-specific enhancer elements (38).

Sox9 is critical to chondrogenesis because it regulates cartilage-specific genes such as *Col2a1*, *Col11a2*, and *Agc1* (7, 10, 11). In addition, Sox9 plays a critical role in testicular development by regulating targets such as *Amh* and *Ptgds* in Sertoli cells (39–41). However, the regulatory mechanism of tissue-specific target distribution is less understood. Previous reports indicated a human SOX9 missense mutation (A76E) in an XY patient exhibiting skeletal abnormalities without sex reversal; this mutation perturbed Sox9 dimerization, resulting in dysregulation of chondrocyte-specific genes (30–32). Sox9 homodimers are believed to bind to enhancer regions containing inverted Sox9 binding sites separated by 3 or 4 bp (30–32). The Sox9 binding site identified in this study is also a Sox9 palindromic binding motif and again indicates that miR-140 is a critical chondrocyte-specific target. In fact, LacZ expression was not detected in the male gonads of any miR140–3k-LacZ Tg embryonic mice (data not shown). We further showed that Sox9 A76E did not up-regulate miR-140 promoter activity even when L-Sox5 and Sox6 were co-expressed. Only one site mutation of the Sox9 palindromic motif completely abolished the ability of the Sox trio to up-regulate promoter activity despite a Sox9 motif mutation that decreased but retained Sox9 binding status. These findings suggest that DNA-dependent Sox9 homodimer formation is needed for L-Sox5 and Sox6 assembly to enhance its DNA binding and/or transactivation ability, but a more detailed mechanism remains undetermined. As previously mentioned, binding of the Sox9 homodimer to its palindromic motif is critical for cartilage-specific gene regulation, and the regulatory mechanism suggested in this study could apply to other cartilage targets. In fact, we observed that Sox9 A76E did not up-regulate luciferase activity from a *Col2a1* enhancer reporter vector with L-Sox5 and Sox6 co-transfection (data not shown).

In conclusion, we report that a proximal region upstream of miR-140 has chondrogenic promoter activity *in vivo*, and its cartilage-specific expression is generated from its transcript within the host gene *Wwp2*. miR-140 promoter activity is up-regulated by the critical transcription factors L-Sox5, Sox6, and Sox9, and their response elements and detailed binding sites were identified. Our findings suggest that the DNA binding and/or transactivation ability of Sox9 in its homodimer form is dependently boosted by L-Sox5 and Sox6.

Acknowledgments—We thank Dr. Makoto Taketo of Kyoto University for the Ck19-Cre mice. We thank Akane Nakamura and Hideki Tsumura for help with generation of miR140–3k-LacZ transgenic mice and Arisa Igarashi and Moe Tamano for technical assistance.

REFERENCES

1. Provot, S., and Schipani, E. (2005) Molecular mechanisms of endochondral bone development. *Biochem. Biophys. Res. Commun.* **328,** 658–665
2. Lefebvre, V., and Smits, P. (2005) Transcriptional control of chondrocyte fate and differentiation. *Birth Defects Res. C Embryo Today* **75,** 200–212
3. Goldring, M. B., Tsuchimochi, K., and Ijiri, K. (2006) The control of chondrogenesis. *J. Cell. Biochem.* **97,** 33–44
4. Akiyama, H., Chaboissier, M. C., Martin, J. F., Schedl, A., and de Crombrugghe, B. (2002) The transcription factor Sox9 has essential roles in successive steps of the chondrocyte differentiation pathway and is required for expression of Sox5 and Sox6. *Genes Dev.* **16,** 2813–2828
5. Akiyama, H., Lyons, J. P., Mori-Akiyama, Y., Yang, X., Zhang, R., Zhang, Z., Deng, J. M., Taketo, M. M., Nakamura, T., Behringer, R. R., McCrea, P. D., and de Crombrugghe, B. (2004) Interactions between Sox9 and β-catenin control chondrocyte differentiation. *Genes Dev.* **18,** 1072–1087
6. Bi, W., Deng, J. M., Zhang, Z., Behringer, R. R., and de Crombrugghe, B. (1999) Sox9 is required for cartilage formation. *Nat. Genet.* **22,** 85–89
7. Bridgewater, L. C., Lefebvre, V., and de Crombrugghe, B. (1998) Chondrocyte-specific enhancer elements in the Col11a2 gene resemble the Col2a1 tissue-specific enhancer. *J. Biol. Chem.* **273,** 14998–15006
8. Han, Y., and Lefebvre, V. (2008) L-Sox5 and Sox6 drive expression of the aggrecan gene in cartilage by securing binding of Sox9 to a far-upstream enhancer. *Mol. Cell. Biol.* **28,** 4999–5013
9. Kou, I., and Ikegawa, S. (2004) SOX9-dependent and -independent transcriptional regulation of human cartilage link protein. *J. Biol. Chem.* **279,** 50942–50948
10. Lefebvre, V., Huang, W., Harley, V. R., Goodfellow, P. N., and de Crombrugghe, B. (1997) SOX9 is a potent activator of the chondrocyte-specific enhancer of the pro-α1(II) collagen gene. *Mol. Cell. Biol.* **17,** 2336–2346
11. Sekiya, I., Tsuji, K., Koopman, P., Watanabe, H., Yamada, Y., Shinomiya, K., Nifuji, A., and Noda, M. (2000) SOX9 enhances aggrecan gene promoter/enhancer activity and is up-regulated by retinoic acid in a cartilage-derived cell line, TC6. *J. Biol. Chem.* **275,** 10738–10744
12. Xie, W. F., Zhang, X., Sakano, S., Lefebvre, V., and Sandell, L. J. (1999) Trans-activation of the mouse cartilage-derived retinoic acid-sensitive protein gene by Sox9. *J. Bone Miner. Res.* **14,** 757–763
13. Smits, P., Li, P., Mandel, J., Zhang, Z., Deng, J. M., Behringer, R. R., de Crombrugghe, B., and Lefebvre, V. (2001) The transcription factors L-Sox5 and Sox6 are essential for cartilage formation. *Dev. Cell* **1,** 277–290
14. Lefebvre, V., Li, P., and de Crombrugghe, B. (1998) A new long form of Sox5 (L-Sox5), Sox6, and Sox9 are coexpressed in chondrogenesis and cooperatively activate the type II collagen gene. *EMBO J.* **17,** 5718–5733
15. Bartel, D. P. (2009) MicroRNAs. Target recognition and regulatory functions. *Cell* **136,** 215–233
16. Cai, X., Hagedorn, C. H., and Cullen, B. R. (2004) Human microRNAs are processed from capped, polyadenylated transcripts that can also function as mRNAs. *RNA* **10,** 1957–1966
17. Lee, Y., Kim, M., Han, J., Yeom, K. H., Lee, S., Baek, S. H., and Kim, V. N. (2004) MicroRNA genes are transcribed by RNA polymerase II. *EMBO J.* **23,** 4051–4060
18. Liu, N., Williams, A. H., Kim, Y., McAnally, J., Bezprozvannaya, S., Sutherland, L. B., Richardson, J. A., Bassel-Duby, R., and Olson, E. N. (2007) An intragenic MEF2-dependent enhancer directs muscle-specific expression of microRNAs 1 and 133. *Proc. Natl. Acad. Sci. U.S.A.* **104,** 20844–20849
19. Rao, P. K., Kumar, R. M., Farkhondeh, M., Baskerville, S., and Lodish, H. F. (2006) Myogenic factors that regulate expression of muscle-specific microRNAs. *Proc. Natl. Acad. Sci. U.S.A.* **103,** 8721–8726
20. Zhao, Y., Samal, E., and Srivastava, D. (2005) Serum response factor regulates a muscle-specific microRNA that targets Hand2 during cardiogenesis. *Nature* **436,** 214–220
21. Tuddenham, L., Wheeler, G., Ntounia-Fousara, S., Waters, J., Hajihosseini, M. K., Clark, I., and Dalmay, T. (2006) The cartilage specific microRNA-140 targets histone deacetylase 4 in mouse cells. *FEBS Lett.* **580,** 4214–4217
22. Miyaki, S., Nakasa, T., Otsuki, S., Grogan, S. P., Higashiyama, R., Inoue, A., Kato, Y., Sato, T., Lotz, M. K., and Asahara, H. (2009) MicroRNA-140 is expressed in differentiated human articular chondrocytes and modulates interleukin-1 responses. *Arthritis Rheum.* **60,** 2723–2730
23. Miyaki, S., Sato, T., Inoue, A., Otsuki, S., Ito, Y., Yokoyama, S., Kato, Y., Takemoto, F., Nakasa, T., Yamashita, S., Takada, S., Lotz, M. K., Ueno-Kudo, H., and Asahara, H. (2010) MicroRNA-140 plays dual roles in both

cartilage development and homeostasis. *Genes Dev.* **24,** 1173–1185
24. Nakamura, Y., He, X., Kato, H., Wakitani, S., Kobayashi, T., Watanabe, S., Iida, A., Tahara, H., Warman, M. L., Watanapokasin, R., and Postlethwait, J. H. (2012) Sox9 is upstream of microRNA-140 in cartilage. *Appl. Biochem. Biotechnol.* **166,** 64–71
25. Yang, J., Qin, S., Yi, C., Ma, G., Zhu, H., Zhou, W., Xiong, Y., Zhu, X., Wang, Y., He, L., and Guo, X. (2011) miR-140 is co-expressed with Wwp2-C transcript and activated by Sox9 to target Sp1 in maintaining the chondrocyte proliferation. *FEBS Lett.* **585,** 2992–2997
26. Yokoyama, S., Hashimoto, M., Shimizu, H., Ueno-Kudoh, H., Uchibe, K., Kimura, I., and Asahara, H. (2008) Dynamic gene expression of Lin-28 during embryonic development in mouse and chicken. *Gene Expr. Patterns* **8,** 155–160
27. Kawakami, Y., Tsuda, M., Takahashi, S., Taniguchi, N., Esteban, C. R., Zemmyo, M., Furumatsu, T., Lotz, M., Belmonte, J. C., and Asahara, H. (2005) Transcriptional coactivator PGC-1α regulates chondrogenesis via association with Sox9. *Proc. Natl. Acad. Sci. U.S.A.* **102,** 2414–2419
28. Barrionuevo, F., Taketo, M. M., Scherer, G., and Kispert, A. (2006) Sox9 is required for notochord maintenance in mice. *Dev. Biol.* **295,** 128–140
29. Yamashita, S., Andoh, M., Ueno-Kudoh, H., Sato, T., Miyaki, S., and Asahara, H. (2009) Sox9 directly promotes Bapx1 gene expression to repress Runx2 in chondrocytes. *Exp. Cell Res.* **315,** 2231–2240
30. Bernard, P., Tang, P., Liu, S., Dewing, P., Harley, V. R., and Vilain, E. (2003) Dimerization of SOX9 is required for chondrogenesis but not for sex determination. *Hum. Mol. Genet.* **12,** 1755–1765
31. Coustry, F., Oh, C. D., Hattori, T., Maity, S. N., de Crombrugghe, B., and Yasuda, H. (2010) The dimerization domain of SOX9 is required for transcription activation of a chondrocyte-specific chromatin DNA template. *Nucleic Acids Res.* **38,** 6018–6028
32. Sock, E., Pagon, R. A., Keymolen, K., Lissens, W., Wegner, M., and Scherer, G. (2003) Loss of DNA-dependent dimerization of the transcription factor SOX9 as a cause for campomelic dysplasia. *Hum. Mol. Genet.* **12,** 1439–1447
33. Baskerville, S., and Bartel, D. P. (2005) Microarray profiling of microRNAs reveals frequent coexpression with neighboring miRNAs and host genes. *RNA* **11,** 241–247
34. Nakamura, Y., He, X., Kobayashi, T., Yan, Y. L., Postlethwait, J. H., and Warman, M. L. (2008) Unique roles of microRNA140 and its host gene WWP2 in cartilage biology. *J. Musculoskelet. Neuronal Interact.* **8,** 321–322
35. Zou, W., Chen, X., Shim, J. H., Huang, Z., Brady, N., Hu, D., Drapp, R., Sigrist, K., Glimcher, L. H., and Jones, D. (2011) The E3 ubiquitin ligase Wwp2 regulates craniofacial development through mono-ubiquitylation of Goosecoid. *Nat. Cell Biol.* **13,** 59–65
36. Saito, T., Ikeda, T., Nakamura, K., Chung, U. I., and Kawaguchi, H. (2007) S100A1 and S100B, transcriptional targets of SOX trio, inhibit terminal differentiation of chondrocytes. *EMBO Rep.* **8,** 504–509
37. Haag, J., Gebhard, P. M., and Aigner, T. (2008) SOX gene expression in human osteoarthritic cartilage. *Pathobiology* **75,** 195–199
38. Bridgewater, L. C., Walker, M. D., Miller, G. C., Ellison, T. A., Holsinger, L. D., Potter, J. L., Jackson, T. L., Chen, R. K., Winkel, V. L., Zhang, Z., McKinney, S., and de Crombrugghe, B. (2003) Adjacent DNA sequences modulate Sox9 transcriptional activation at paired Sox sites in three chondrocyte-specific enhancer elements. *Nucleic Acids Res.* **31,** 1541–1553
39. Arango, N. A., Lovell-Badge, R., and Behringer, R. R. (1999) Targeted mutagenesis of the endogenous mouse Mis gene promoter. *In vivo* definition of genetic pathways of vertebrate sexual development. *Cell* **99,** 409–419
40. De Santa Barbara, P., Bonneaud, N., Boizet, B., Desclozeaux, M., Moniot, B., Sudbeck, P., Scherer, G., Poulat, F., and Berta, P. (1998) Direct interaction of SRY-related protein SOX9 and steroidogenic factor 1 regulates transcription of the human anti-Müllerian hormone gene. *Mol. Cell. Biol.* **18,** 6653–6665
41. Wilhelm, D., Hiramatsu, R., Mizusaki, H., Widjaja, L., Combes, A. N., Kanai, Y., and Koopman, P. (2007) SOX9 regulates prostaglandin D synthase gene transcription *in vivo* to ensure testis development. *J. Biol. Chem.* **282,** 10553–10560

軟骨細胞分化における miRNA

浅原 弘嗣*

マイクロRNAはノンコーディングRNAの一種であり，20～25塩基ほどの1本鎖RNAである。ターゲットとなる遺伝子のmRNAに結合し，その発現を抑制する機能を持ち，発生，がん，炎症などあらゆる医学・生物学分野において重要な役割を担うことが明らかにされてきている。
本稿では，特に軟骨細胞および関節軟骨組織の発生，および恒常性維持におけるmiRNAの機能を紹介する。

Frontier of epigenome in bone research.

miRNAs in cartilage development.

Department of Systems BioMedicine, Tokyo Medical and Dental University/
Department of Systems BioMedicine, National Research Institute for Child Health and Development, Japan.

Hiroshi Asahara

MicroRNAs (miRs) are ～22 nucleotide non-cording forms of RNA and exhibit tissue or developmental stage specific expression patterns. Recent findings show taht the expression of miR-140, which is specifically expressed in chondrocytes, is reduced in OA chondrocytes. Furthermore, knockdown of miR-140 in mice chondrocytes promotes arthritis in mice. In addition to this, several other miRs have also been shown to play important roles in chondrocytes. Thus, miRs should be critical factors for cartilage development and homeostasis.

はじめに

マイクロRNAはノンコーディングRNAの一種であり，20～25塩基ほどの1本鎖RNAである。ターゲットとなる遺伝子のmRNAに結合し，その発現を抑制する機能を持ち，発生，がん，炎症などあらゆる医学・生物学分野において重要な役割を担うことが明らかにされてきている。

骨・軟骨の発生におけるmiRNAの重要性

通常のmRNAと同様，miRNAはまず数百一数千塩基長のpri-miRNA (primary microRNA) として転写され，さらに，その転写物がいくつかのス

*東京医科歯科大学医歯学総合研究科システム発生・再生医学分野・教授/国立成育医療研究センター研究所・客員研究部長
（あさはら・ひろし）

テップを経て成熟型の機能を持つmiRNAとなる。

核内でまず酵素DroshaとDGCR8により，stem-loop構造の70塩基程度のpre-miRNA (precursor miRNA)に切り出され，さらにそれがExportin-5によって細胞質に運ばれ，DicerおよびTRBP/PACT (transactivation-response element RNA-binding protein/protein activator of the interferon-induced protein kinase)により，20～25塩基のmiRNAを含む2本鎖RNAが生成される。この2本鎖RNAのうちmiRNA側のみがRISC (RNA-induced silencing complex)に結合することで，機能的 (mature) miRNA-RISC複合体となる[1)2)]。

このようなプロセスにおいてDicerは，ほぼすべてのmiRNA生成に不可欠である。しかし，そのノックアウトマウスは胎生期7.5日で死亡するため[3)]，各組織におけるmiRNAの機能研究では，それぞれの組織におけるコンディショナルなDicerノックアウトマウスの解析が行われてきた。

Tabinらは，胎芽全域で特異的にCreを発現するPrx-CreマウスとDicer-Floxマウスを掛け合わせて，四肢特異的なDicerコンディショナルノックアウトマウスを作製し，このマウスの四肢における骨形成は，骨形成パターン自体は保たれていたものの，四肢の短小化がみられることを報告し，軟骨・骨形成においてmiRNAが重要であることを示唆した[4)]。

さらに，内軟骨性骨化初期での軟骨誘導におけるmiRNAの機能研究では，Kronenbergらは，Col2-CreマウスとDicer-Floxマウスを掛け合わせて軟骨特異的なmiRNAノックアウトマウスを作製し[5)]，このマウスには，内軟骨性骨化における軟骨の増殖が減少した結果，肥大軟骨細胞への移行が早まり，骨格の短小化が起きていることを報告した[5)]。このように，軟骨発生分化においてもmiRNAが重要であることが明らかとなった。

軟骨特異的な発現を示すmiRNA

発生期に組織特異的な発現をするmiRNAをシステマティックに解析する目的で，ゼブラフィッシュをモデルにホールマウントインサイチューハイブリダイゼーション (whole mount *in situ* hybridization：WISH)を行った。結果，軟骨に発現を示すものについては，ユビキタスに発現するもの以外に，miR-146，140*，199a，199a*，145の報告がある[6)]。その中でも，140，199a，199a*については，メダカや，ニワトリでも軟骨での発現が報告されている[7)]。特に，miR-140は他の組織では発現が低く，軟骨のみに特異的な発現を示すことが，マウス胎児を用いたWISHによっても報告された[8)]。199a，199a*については，small RNAのライブラリースクリーニングでマウス結合組織での発現が確認されている。miR-140の軟骨における機能については，ゼブラフィッシュを用いた解析においてplatelet-derived growth factor (PDGF)シグナルを介する軟骨分化制御機構が確認された[9)]。

軟骨細胞に特異的に働くmiRNAを同定するため，われわれは，ヒト関節軟骨を用いたmiRNAに対するマイクロアレイ解析を行い，軟骨分化におけるmiR-140のより特異的な発現上昇を確認している[10)]。また，miR-140の発現はMSCsの軟骨分化と正相関し，分化に伴ってSox9，Col2a1のような軟骨分化マーカーと同じ発現増加を示すことも明らかとなった。

miR-140と発生・軟骨ホメオスタシス (図)

miR-140は正常ヒト関節軟骨で高い発現を示

pri-miRNA：primary microRNA，pre-miRNA：precursor miRNA
TRBP/PACT：transactivation-response element RNA-binding protein/protein activator of the interferon-induced protein kinase，RISC：RNA-induced silencing complex，WISH：whole mount *in situ* hybridization
PDGF：platelet-derived growth factor (血小板由来増殖因子)

す一方，変形性関節症（OA）軟骨においてはその発現量は有意に低下しており，IL1-βによる関節軟骨細胞刺激においてもmiR-140の発現は低下することが確認された[10]。これらの結果から，miR-140の発現低下がOAにおける病的な遺伝子発現の誘因となっており，miR-140がOAの病態と関連していることが示唆される[10]。

そのためわれわれは，miR-140ノックアウトマウスとトランスジェニックマウスを作製し，miR-140の機能解析を行った。結果，miR-140ノックアウトマウスは発生異常は認められなかったものの，生後，四肢，体幹，顔面の短小化がみられ，Dicerノックアウトマウスでみられた表現型の一部がmiR-140で説明できることを確認した[11]。

同様の表現型は，われわれとは別のmiR-140ノックアウトマウスでも報告されている[12]。これらの結果から，miR-140が内軟骨性骨成長に不可欠であり，Dnpepを介したbone morphogenetic protein（BMP）シグナル抑制が，その原因の一つとして考えられた。

また，肢芽のマイクロマスカルチャーにおけるmiR-140ノックダウン解析では，BMPシグナルの下流で働くSp1によって軟骨細胞増殖が低下することが報告されており[13]，miR-140が内軟骨性骨成長において，Dnpep，SP1，BMP2といった複数の遺伝子をターゲットとして働いていることが明らかとなった。早期のOAでは関節軟骨の変化のみならず，軟骨下骨の肥厚，柔軟性の

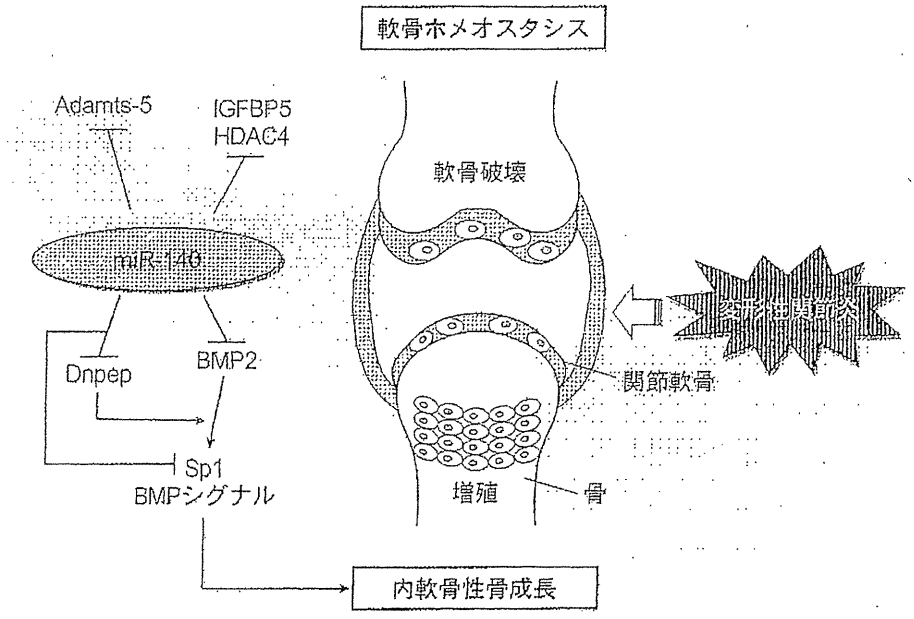

図　miR-140を介した軟骨発生・代謝制御機構

miR-140は，異なるターゲットを制御することで，内軟骨骨化と軟骨ホメオスタシスの両方を調節することができる。

BMP：bone morphogenetic protein，HDAC4：histone deacetylase 4，IGFBP5：insulin-like growth factor binding protein 5

（文献11より）

OA：osteoarthritis（変形性関節症），BMP：bone morphogenetic protein，AIA：antigen-induced arthritis
HDAC4：histone deacetylase 4（ヒストン脱アセチル化酵素4）
IGFBP5：insulin-like growth factor binding protein 5（インスリン様増殖因子結合タンパク質5）

低下，骨梁の減少なども起きており，OA軟骨におけるmiR-140の発現の低下が，BMPシグナルを介して軟骨下骨の変性にも関与していることが示唆される。これらの変性によるストレスの増加が，関節軟骨の変性を促進させOAの進行につながっているとする報告もある[14]。

軟骨ホメオスタシスにおけるmiR-140の役割を明らかにするため，時間軸でのmiR-140の変化を調べた結果，膝関節軟骨は生後1カ月まで正常であったが，3カ月以降は徐々にプロテオグリカンの減少や軟骨のフィブリレーションなどのOAの進行が確認された。また，サージカルOAモデルにおいても，miR-140ノックアウトマウスは術後8週でwild typeマウスと比べ有意にOAの進行が確認された。さらにmiR-140の軟骨変性への効果を調べるため，wild typeマウス，miR-140ノックアウトマウス，miR-140トランスジェニックマウスそれぞれの膝関節にantigen-induced arthritis (AIA) モデルを作製した結果，miR-140トランスジェニックマウスではプロテオグリカンとtype-Ⅱ collagenの減少に対する抵抗性が確認され，miR-140が炎症による軟骨変性に対して予防効果を持つことが示唆された[11]。miR-140が，OAの主要なプロテアーゼであるAdamts-5を直接の標的分子として抑制することがこの理由の一つであるが，軟骨細胞においてmiR-140によって抑制されると報告されているHDAC4 (histone deacetylase 4)，IGFBP5 (insulin-like growth factor binding protein 5) やBMPシグナルなどもこの結果の一因となっていると考えられる[10]~[14]。このようにmiR-140は，複数のpathwayにおいて多数の遺伝子をターゲットにしていることが明らかとなってきており，軟骨実質の生成や分解を調節し，軟骨のホメオスタシスを維持する主要なmiRNAであると言える。

おわりに

miR-140による軟骨治療は，早期のOAに対して理想的な治療薬となる可能性を秘めており，今後の研究が期待される。

文　献

1) Carthew RW, Sontheimer EJ：Origins and mechanisms of miRNAs and siRNAs. Cell 136：642-655, 2009.
2) Siomi H, Siomi MC：On the road to reading the RNA-interference code. Nature 457 (7228)：396-404, 2009.
3) Bernstein E, Kim SY, Carmell MA, et al：Dicer is essential for mouse development. Nat Genet 35：215-217, 2003.
4) Harfe BD, McManus MT, Mansfield JH, et al：The RNase Ⅲ enzyme Dicer is required for morphogenesis but not patterning of the vertebrate limb. Proc Natl Acad Sci U S A 102 (31)：10898-10903, 2005.
5) Kobayashi T, Lu J, Cobb BS, et al：Dicer-dependent pathways regulate chondrocyte proliferation and differentiation. Proc Natl Acad Sci U S A 105 (6)：1949-1954, 2008.
6) Wienholds E, Kloosterman WP, Miska E, et al：MicroRNA expression in zebrafish embryonic development. Science 309：310-311, 2005.
7) Ason B, Darnell DK, Wittbrodt B, et al：Differences in vertebrate microRNA expression. Proc Natl Acad Sci U S A 103：14385-14389, 2006.
8) Tuddenham L, Wheeler G, Ntounia-Fousara S, et al：The cartilage specific microRNA-140 targets histone deacetylase 4 in mouse cells. FEBS Lett 580：4214-4217, 2006.
9) Eberhart JK, He X, Swartz ME, et al：MicroRNA Mirn140 modulates Pdgf signaling during palatogenesis. Nat Genet 40：290-298, 2008.
10) Miyaki S, Nakasa T, Otski S, et al：MicroRNA-140 is expressed in differentiated human articular chondrocytes and modulates IL-1 re-

sponses. Arthritis Rheum 60 (9) : 2723-2730, 2009.
11) Miyaki S, Sato T, Inoue A, et al : MicroRNA-140 plays dual roles in both cartilage development and homeostasis. Genes Dev 24 : 1173-1185, 2010.
12) Nakamura Y, Inloes JB, Katagiri T, Kobayashi T : Chondrocyte-specific microRNA-140 regulates endochondral bone development and targets Dnpep to modulate bone morphogenetic protein signaling. Mol Cell Biol 31 : 3019-3028, 2011.
13) Yang J, Qin S, Yi C, et al : MiR-140 is co-expressed with Wwp2-C transcript and activated by Sox9 to target Sp1 in maintaining the chondrocyte proliferation. FEBS Lett 585 : 2992-2997, 2011.
14) Araldi E, Schipani E : MicroRNA-140 and the silencing of osteoarthritis. Genes Dev 24 : 1075-1080, 2010.

BMC Musculoskeletal Disorders

RESEARCH ARTICLE Open Access

Decreased Semaphorin3A expression correlates with disease activity and histological features of rheumatoid arthritis

Shu Takagawa[1], Fumio Nakamura[2*], Ken Kumagai[1], Yoji Nagashima[3], Yoshio Goshima[2] and Tomoyuki Saito[1*]

Abstract

Background: Rheumatoid arthritis (RA) is an autoimmune disease of which the pathogenetic mechanisms are not fully understood. Semaphorin3A (Sema3A) has an immune regulatory role. Neuropilin1 (NRP1), the primary receptor for Sema3A, is also a receptor for vascular endothelial growth factor 165 ($VEGF_{165}$). It has been shown that Sema3A competitively antagonizes VEGF165 signaling. This study investigated whether Sema3A is expressed in synovial tissues, and is associated with disease activity and the histological features of synovial tissues from RA patients.

Methods: Human synovial tissues samples were obtained from RA and osteoarthritis (OA) patients. Disease activity of RA patients was calculated using the 28-joint Disease Activity Score based on C-reactive protein (DAS28-CRP). The histological features of RA synovial tissues were evaluated using Rooney's inflammation scoring system. The localization of Sema3A, $VEGF_{165}$ and NRP1 positive cells was immunohistochemically determined in synovial tissues. Expression levels of *Sema3A, VEGF-A* and *NRP1* mRNA were determined using quantitative real-time polymerase chain reaction (qPCR).

Results: In OA specimens, Sema3A, $VEGF_{165}$ and NRP1 proteins were expressed in the synovial lining and inflammatory cells beneath the lining. Immunohistochemistry revealed the protein expression of Sema3A in synovial lining cells was decreased in RA tissues compared with OA samples. qPCR analysis demonstrated a significant reduction of *Sema3A* mRNA levels in RA synovial tissue samples than in OA and a significant correlation of the ratio of *Sema3A/VEGF-A* mRNA expression levels with DAS28-CRP ($R = -0.449$, $p = 0.013$). *Sema3A* mRNA levels also correlated with Rooney's inflammation score, especially in perivascular infiltrates of lymphocytes ($R = -0.506$, $p = 0.004$), focal aggregates of lymphocytes ($R = -0.501$, $p = 0.005$) and diffuse infiltrates of lymphocytes ($R = -0.536$, $p = 0.002$).

Conclusions: Reduction of Sema3A expression in RA synovial tissues may contribute to pathogenesis of RA.

Keywords: Rheumatoid arthritis, Semaphorin3A, Disease activity score, Histological scoring

Background

Rheumatoid arthritis (RA) is a chronic inflammatory disease characterized by progressive joint destruction that accompanies the proliferation of synovial cells and blood vessels as well as invasion of inflammatory cells [1-3]. Although the initiating factors of RA are unknown, autoimmune reactions are activated in connective tissues. In RA joints, immune cells such as T and B cells invade the hyperplastic synovial membranes [4]. Activated synovial T and B cells secrete various types of pro-inflammatory cytokines including interleukin-1 (IL-1), IL-17 and tumor necrosis factor-α (TNF-α). These cytokines induce the synthesis of matrix degrading enzymes in chondrocytes. Synovial fibroblasts also produce matrix-degrading enzymes and can invade cartilage, leading to its destruction [3,4].

Semaphorins are a large family of proteins that function as guidance cues for axonal/dendritic projections. Class 3 semaphorins are vertebrate secreted proteins and include seven members, semaphorin3A (Sema3A) to Semaphorin3G (Sema3G) [5]. Sema3A is a repulsive

* Correspondence: f-nakamura@umin.ac.jp; t_saito@med.yokohama-cu.ac.jp
[2]Department of Molecular Pharmacology and Neurobiology, Yokohama City University Graduate School of Medicine, 3-9 Fukuura, Kanazawa-ku, Yokohama 236-0004, Japan
[1]Department of Orthopaedic Surgery, Yokohama City University Graduate School of Medicine, 3-9 Fukuura, Kanazawa-ku, Yokohama 236-0004, Japan
Full list of author information is available at the end of the article

factor for sensory fibers, and Semaphorin3C (Sema3C) and Semaphorin3F (Sema3F) repulse sympathetic nerve fibers [6]. Whereas the primary receptor for Sema3A is neuropilin1 (NRP1), Sema3F has a higher binding affinity to neuropilin2 (NRP2). Sema3C binds to both NRP1 and NRP2 [7,8].

The action of Sema3A is not limited to the nervous system as NRP1 is expressed on endothelial cells, keratinocytes, T cells, and tumor cells in breast and prostate cancer. Sema3A inhibits angiogenesis, migration of keratinocytes, proliferation of T cells, and migration of tumor cells [8-11]. In addition, it was recently shown that Sema3A is involved in the entry of dendritic cells to the lymphatic system [12]. Several studies have indicated that a reduction of Sema3A expression is involved in the exacerbation of autoimmune diseases, such as RA and systemic lupus erythematosus (SLE) [13,14].

NRP1 mediates signal transduction through PlexinA coreceptors [15], which are classified into four sub-families, PlexinA1–4 [16]. The Sema3A/NRP1/PlexinA complex regulates the actin cytoskeleton through small G-proteins, including Rac and Rho [17]. In immune cells, the Rac family is associated with the proliferation and activation of B cells [18], and the activation of T cells induced by dendritic cells [19]. NRP1 is also a putative marker of regulatory T cells [20], and therefore Sema3A/NRP1/PlexinA signaling may modulate regulatory T cell functions.

Vascular endothelial growth factor165 ($VEGF_{165}$), a spliced isoform of VEGF-A [21], binds to NRP1 [22]. VEGF is a key regulator of angiogenesis and is involved in the development of inflammation [23]. In RA patients, serum VEGF levels positively correlate with disease activity score and joint destruction [24,25]. Because NRP1 is a common receptor for Sema3A and $VEGF_{165}$ [11,26], the efficacy of $VEGF_{165}$ is attributed to Sema3A expression. Indeed, the imbalance between Sema3A and VEGF expression levels is also associated with disease activity in several tumors [27-29].

These facts prompted us to investigate the possibility that Sema3A expression and/or the balance of Sema3A and $VEGF_{165}$ expression may regulate the disease activity of RA including inflammation, angiogenesis and proliferation of synovial cells. We found that Sema3A expression was decreased in RA synovial tissues when compared with osteoarthritis (OA) samples. The Sema3A expression level was also significantly associated with the RA pathological score and disease activity score.

Methods

Patients and samples

Synovial tissue samples were obtained from RA (n = 30) and OA (n = 23) patients during total knee arthroplasty. The diagnosis of patients with RA and OA was based on the revised 1987 American Rheumatism Association Criteria for RA [30] and the American Rheumatism Association Criteria for OA [31], respectively, as shown in Table 1. Before arthroplasty, the disease activity of each RA patient was evaluated using the 28-joint Disease Activity Score based on C-reactive protein (DAS28-CRP) [30,32]. This study was approved by the Ethics Committee of Yokohama City University Graduate School of Medicine, and written informed consent was obtained from all patients involved in this study (notice of approval Institutional Review Board protocol number: B1100513031).

Hematoxylin and eosin (HE) staining for histological assessment

Tissue specimens were fixed with 20% formalin and embedded in paraffin. Paraffin sections (4 μm thick) were stained with HE. The histological features of RA synovial tissues were evaluated using Rooney's inflammation scoring system [33]. These histological parameters included the degree of synovial hyperplasia, fibrosis, the number of blood vessels, focal and diffuse aggregates of lymphocytes and perivascular infiltrates of lymphocytes. All parameters were scored separately on a scale of 0–10 (Table 2). Two investigators (S.T. and Y.N.) independently assessed the histologic severity.

Immunohistochemistry

For immunostaining of Sema3A, antigen retrieval was performed by incubating at 95°C for 30 min in DAKO Target Retrieval Solution (pH 9.0; DAKO, Glostrup, Denmark). For immunostaining of NRP1, $VEGF_{165}$, CD3 and CD20, the tissue sections were subjected to antigen retrieval by autoclaving in 10 mM citrate buffer (pH 6.0) for 15 min at 121°C. Slides were then treated with 0.3% H_2O_2 for 30 min to block endogenous peroxidases. Sections for Sema3A, NRP1 and $VEGF_{165}$ staining were blocked with 10% normal goat serum. All sections were incubated at 4°C overnight with rabbit anti-Sema3A polyclonal antibody (1:200; Abcam, Cambridge, UK), mouse anti-CD3 monoclonal antibody (1:50; DAKO), mouse anti-CD20 monoclonal antibody (DAKO), rabbit anti-NRP1 polyclonal antibody (1:100; Santa Cruz Biotechnology, Santa Cruz, CA, USA) or rabbit anti-$VEGF_{165}$ polyclonal antibody (1:100; Millipore, MA, USA). This was followed by incubation with Envision™, Rabbit/HRP (DAKO) for Sema3A, NRP1 and $VEGF_{165}$ or Envision™/HRP (DAKO) for CD3 and CD20. Immunoreactivity was visualized using 3,3'-diaminobenzidine plus (DAB+, DAKO) for Sema3A, NRP1 and $VEGF_{165}$, or 3,3'-diaminobenzidine tetrahydrochloride (DAB; Sigma-Aldrich, St. Louis, MO, USA) for CD3 and CD20. Finally, the sections were counterstained with hematoxylin and mounted. Controls for Sema3A immunohistochemistry included preabsorption and co-incubation of the antibody with the antigen peptide (1 μl/ml; Abcam).